UNIVERSITY OF CALIFORNIA,
IRVINE

Characteristics of EEG-based Brain Connectivity in Infantile Spasms Patients with Hypsarrhythmia

THESIS

submitted in partial satisfaction of the requirements
for the degree of

MASTER OF SCIENCE

in Biomedical Engineering

by

Vaibhav Bajaj

Thesis Committee:
Professor Beth Lopour, Chair
Professor Frithjof Kruggel
Professor Jack J Lin

2015

DEDICATION

To

my parents: Avinash and Anupam Bajaj

my sister: Shivani Bajaj

my motivator and dearest person in my life: Brittany P Lim

TABLE OF CONTENTS

	Page
LIST OF FIGURES	v
LIST OF TABLES	vi
ACKNOWLEDGMENTS	vii
ABSTRACT OF THE THESIS	viii
INTRODUCTION: 1. Background	1
2. Previous Work	2
3. Objective	3
CHAPTER 1: Methods	
1. Subjects	5
2. EEG Recording	5
3. Cross Correlation Analysis	6
4. Resolving Volume Conduction and Common Average Effects	8
5. Partial Cross Correlation	8
6. Non-Parametric Permutation Testing	10
7. Non-Parametric Determination of Significant Edges for Visualization	11
8. Individual Patient Analysis of Network Stability	12
9. Histogram of Hypsarrhythmia and Non-Hypsarrhythmia Patients	13
10. Electrode Distance compared to Cross Correlation Values	14
11. Statistics Comparing Hypsarrhythmia and Non-Hypsarrhythmia Patients	15
CHAPTER 2: Results	
1. Visualization of Connectivity Results	16
2. Stability of Connectivity is Shown with Increased Temporal Window	21
3. Distributions of Hypsarrhythmia and Non-Hypsarrhythmia Patients Show Significance	24
4. Electrode Distance to Average Connectivity shows Higher Connectivity Values in Hypsarrhythmia Patients	26
5. Statistical Results on Comparison of Groups of Patients	29
CHAPTER 3: Discussion	
1. Connectivity Analysis Reveals Unique Networks across Subjects	34
2. Network Stability More Stable with Increasing Temporal Window Size	35
4. Statistical Analysis on Distance Displays Significance for Long Range Connections	35
5. Analysis on Hypsarrhythmia and Non-Hypsarrhythmia Patients	36

CHAPTER 4: Future Work
1. More Patients Needed 39
2. Eyeblink and Eye Movement Calculations 39
3. Graph Theory 40
4. More Processes to Differentiate Hypsarrhythmia and Non-Hypsarrhythmia 41

REFERENCES 42

Supplementary Figures 45

LIST OF FIGURES

		Page
Figure 1	Difference between Cross Correlation and Partial Correlation	9
Figure 2	Distribution of Non-Parametric Maximum Values	11
Figure 3	Connectivity Heat Map of two Hypsarrhythmia Patients	17
Figure 4	Connectivity Heat Map of two Non-Hypsarrhythmia Patients	18
Figure 5	Brain Map of two Hypsarrhythmia Patients	19
Figure 6	Brain Map of two Non-Hypsarrhythmia Patients	20
Figure 7	Network Stability by Average Change in State 1A	22
Figure 8	Network Stability by Average Change in State 1S	22
Figure 9	Network Stability by Average Change in State 2A	23
Figure 10	Network Stability by Average Change in State 2S	23
Figure 11	Histogram plot Depicting the $\bar{\rho}_{ij}$without Zero Value Connectivity	25
Figure 12	Scatter Plot of $\bar{\rho}_{ij}$ relative to distance for State 1A	27
Figure 13	Scatter Plot of $\bar{\rho}_{ij}$ relative to distance for State 1S	27
Figure 14	Scatter Plot of $\bar{\rho}_{ij}$ relative to distance for State 2A	28
Figure 15	Scatter Plot of $\bar{\rho}_{ij}$ relative to distance for State 2S	28
Supplementary Figure 1	Connectivity Heat Map of Hypsarrhythmia Patients	55
Supplementary Figure 2	Connectivity Heat Map of Non-Hypsarrhythmia Patients	56
Supplementary Figure 1	Brain Map of Hypsarrhythmia Patients	57
Supplementary Figure 2	Brain Map of Non-Hypsarrhythmia Patients	58

LIST OF TABLES

		Page
Table 1	Patient Sample Size	5
Table 2	KS-Test on Distributions of Connectivity Values	26
Table 3	ANOVAN statistical Results on Distances and Cross-Connectivity	31
Table 4	ANOVAN and Paired T-test on Group Comparisons	32
Table 5	Paired T-Test on Responders and Non-Responders	33

ACKNOWLEDGMENTS

I would like to express the deepest appreciation to my committee chair, Professor Beth Lopour, who has been a great mentor and taken the time to direct me in the pursuit of my degree.

I would like to thank my committee members, Professor Frithjof Kruggel and Professor Jack J Lin, for their support and guidance in my thesis.

In addition, I would like to thank, Dr. Daniel W Shrey, who has taken the time to retrieve patient data, select the data sets to work with, and analyzed all data sets for artifacts.

I would like to give a special thanks to Darren Weber, who created the elec_distance file for calculating spherical arc length.

Also, I would like to thank everyone in the Lopour Laboratory for giving me advice into my project.

ABSTRACT OF THE THESIS

Characteristics of EEG-based Brain Connectivity in Infantile Spasms Patients with Hypsarrhythmia

By

Vaibhav Bajaj

Master of Science in Biomedical Engineering

University of California, Irvine, 2015

Professor Beth Lopour, Chair

An infantile spasms syndrome is a subset of epileptic syndrome occurring in children less than two years old. Approximately two-thirds of these patients have hypsarrhythmia, whose EEG patterns display large amplitudes, multifocal sharp waves, and described as disorganization. However, there are many variations of hypsarrhythmia, and the criteria for recognizing hypsarrhythmia vary across clinicians, leading to a need for a differentiable pattern among the clinically diagnosed hypsarrhythmia patients and those without hypsarrhythmia. Patients in this study had recorded EEG of the pre- and post- treatment in both awake and sleep states. The EEG data of these patients underwent a connectivity analysis using maximum cross correlations among electrode pairs. Previous research has shown EEG connectivity leads to unique connectivity and network stability in adult patients. We incorporated these techniques to study the brain networks of children with infantile spasms. More specifically, we wanted to focus on spatial distributions of connectivity, statistical analysis on connectivity, and network stability. From our analysis, there is a statistical difference between spatial distributions of connectivity in patients of hypsarrhythmia and non-hypsarrhythmia across all states. Furthermore, there is a statistical increase in long range connections for hypsarrhythmia patients in the sleep states, both

pre- and post- treatment. We are also able to note network stability with increasing temporal window size, but more stability in the pre- than post-treatment and in the sleep than awake state. This analysis is intriguing because the disorganization of hypsarrhythmia may lead to assume the networks are not stable over long periods of time.

INTRODUCTION

1. Background

Infantile spasms syndrome is a clinically diagnosed epileptic syndrome occurring in children less than 2 years of age [1]. Common diagnostic resources include MRI scans, EEG readings, physical examinations, and medical history examinations [2]. Infantile spasms are characterized by brief contractions followed by less intense contractions lasting up to 2 seconds, which involves flexor, extensor, or mixed spasms in the muscles of neck, trunk, and legs. The more characteristic movements involve flexor spasms involving the head and raising of arms [1]. Approximately two-thirds of infantile spasm patients have hypsarrhythmia [3]. Hypsarrhythmia patients have an underlying abnormal EEG patterns of "large amplitude slow waves mixed with single, multifocal spikes and sharp waves," and disorganized EEG [1]. There are patients with infantile spasms that do not have this characteristic hypsarrhythmia [4].

Patients with infantile spasms have a greater risk towards mental retardation, chronic epilepsies, and other neurodevelopmental disabilities [1]. Current treatment includes high doses of adrenocorticotropic hormone, prednisone, or vigabatrin, which have had a high rate of success [1, 5]. Although there is a high success rate in treatments, the underlying neural activity that generates this characteristic pattern is unknown. Furthermore, there are many variations of hypsarrhythmia, which some are easily definable and some are not [1, 4, 6, 7]. Clinicians may diagnose certain infantile spasm patients differently due to the wide variation in EEG patterns and varied criteria for diagnosis [1]. Thus, there is a greater need to define a differentiable pattern among hypsarrhythmia patients. Based on clinical readings of EEG by epileptologists, disorganized patterns of EEG are seen in hypsarrhythmia patients, leading to the belief that there

is lack of consistent networks within hypsarrhythmia patients. However, there has been little analysis conducted on the EEG patterns in hypsarrhythmia patients.

2. Previous Work

Previous research on connectivity in hypsarrhythmia patients with EEG has been conducted by Burroughs et al [8]. In their research, they had compared hypsarrhythmia connectivity to healthy infants over various frequency bands, and had found that enhanced coherence existed more in hypsarrhythmia patients than healthy.

Other research has tried to classify default mode networks in human adults using fMRI studies for the sleep and awake states, and have found more persistent networks during the sleep states, which can be tested with our research as well [9, 10]. Functional brain networks have been conducted on high-density EEG patients, aged 2-6, displaying stronger connectivity in older children than younger children, and that there are sub-networks of interconnected regions that have edge weights that remain stable over age as calculated by graph theory measures [11].

Chu et al. conducted an experiment to view the persistent 5% connections through EEG patterns on five healthy adults, which found results in having unique and persistent networks in healthy adult EEG [6]. The procedures used by Chu et al were based off of Kramer et al., who developed a procedure for connectivity analysis with EEG examples, which we believe was the strongest approach for connectivity procedures [14, 15]. In these methods, One second windows of EEG data with zero mean and unit variance were used for analysis over the broadband spectrum (0.5-55 Hz). To calculate electrode associations, a maximal cross-correlation between the pairs of electrodes with a lag of 200ms was incorporated. The result from these average strength electrode associations are persistent networks that display uniqueness among all

patients, in that there is no consistency among all 5 patients' networks. Also, Chu et al. incorporated a functional network stability based on epoch length and cross correlations, determining that cross correlation values begin to stabilize at greater than 100 seconds. These results act as a measure of comparison for the EEG data retrieved and analysis conducted on infantile spasm patients. Furthermore, the set of procedures used by Chu et al. and Kramer et al. can be directly incorporated into our project as the similarities exist in using EEG data and dealing with volume conduction effects to produce networks based on strength of cross correlation values.

Similar sets of procedures have been incorporated and proven useful for defining EEG functional connectivity in underlying white matter [12] and in a connectivity analysis for deception tasks [13] that gives value to incorporating these sets of procedures.

Previous research has been conducted comparing connectivity of electrodes with entropy and correlation dimension. In these works, the research was able to display that high connectivity or coherence of electrodes is related to lower entropy and dimension, which is predominantly in sleep states and interictal regions of seizures. Also, research showed that low connectivity or coherence of electrodes is related to higher entropy and higher correlation dimensionality, which is primarily in awake states [16, 17, 18].

3. Objective

We expect, using the connectivity analysis procedures, that there will be a significant difference among the connectivity distributions of those with hypsarrhythmia versus those that have spasms but not hypsarrhythmia due to the disorganized nature of EEG in hypsarrhythmia patients. We further expect that hypsarrhythmia patients will have a greater number of long

range connections relative to non-hypsarrhythmia patients due to the global spread of EEG with high amplitudes and disorganization. Furthermore, we would see stronger connectivity and greater network stability in the post- than pre- treatments and in the sleep states than awake.

Chapter 1: Methods

1. Subjects

We studied 14 patients aged 1-2 years. Of these, 10 patients were treated at the University of California, Los Angeles (UCLA) Medical Center and 4 were treated at Children's Hospital Orange County (CHOC). All EEG data was recorded and collected in accordance with study protocols approved by the Medical Institutional Review Boards at UCLA and CHOC, respectively. All patients were diagnosed with infantile spasms, and 10 were determined to have changes in the background EEG rhythm consistent with hypsarrhythmia (H). We will refer to the other 4 patients as non-hypsarrhythmia (NH). The 14 patients were treated with prednisone, adrenocorticotropic hormone, or vigabatrin. Three of the patients were given the drug treatments but post analysis indicated that their spasms and hypsarrhythmia continued. Two patients did not have a post-treatment EEG recording. Table 1 describes these patients, and in parenthesis are the electrode pairs available for connectivity comparison.

Patient Sample Size (Total Electrode Pairs)				
	Responders	Non-Responders	Pre-Only	Total
Hypsarrhythmia (H)	7 (1197)	2 (342)	1	10
Non-hypsarrhythmia (NH)	3 (513)	0 (0)	1	4

Table 1. A table based visualization of the patient sample size within each group. Outside of parentheses is the patient sample size and within the parentheses is the total number of electrode connectivity pairs.

2. EEG Recording

EEG was recorded using a 10-20 electrode system during both awake (A) and sleep (S) states within the pre- (1) and post- (2) treatment periods. The recording used 23 electrodes at a

sampling rate of 200Hz. A pediatric epileptologist, board certified in neurology, viewed the recordings and selected the cleanest 20 minutes of EEG signal for each patient in each of the four states. Additionally, the epileptologist went through each of the 20 minute segments to identify time periods for which there were high artifact remnants and/or additional noisy electrodes to be removed for each patient. When an artifact was identified (even in a single electrode channel), the time periods were removed across all channels to prevent any effect on the analysis.

For all patients and states, we removed electrodes T2, T1, A2, and A1 because these electrodes contained high frequency noise due to muscle artifact and movement. This resulted in a total of 19 electrodes that could be analyzed, which were Fp2, F4, C4, P4, O2, F8, T8, P8, Fz, Cz, Pz, Fp1, F3, C3, P3, 01, F7, T7, and P7. Therefore, each dataset consisted of a maximum of 19 channels of EEG recorded for 20 minutes.

3. Cross Correlation Analysis

Connectivity measures were calculated in MATLAB using broadband data (0.5 Hz to 55 Hz) with a process adapted from Chu et al [14, 15]. For each patient and specific state, the EEG referential (REF) data and the corresponding time were extracted. Furthermore, all artifacts and noisy channels, as noted by the epileptologist, were removed. Because the connectivity analysis was calculated on successive one-second intervals, any one-second interval that contained any portion of an artifact was removed. Additionally, all trailing zeros in the dataset were removed. With the artifacts removed, we implemented a common average reference, where the mean of all channels at a given time point was subtracted from each channel. We used a third order butterworth filter on the EEG data to obtain a broadband power spectrum between 0.5 Hz and 55 Hz.

Connectivity was calculated in one-second intervals [15], equivalent to 200 data points. Within the one second interval, each channel was ensured to have zero mean and unit variance. We first calculated the biased cross correlation between all channel pairs $x_i[t]$ and $x_j[t]$ for a given lag τ [14]:

$$CC_{ij}[\tau] = \frac{1}{N}\sum_{t=1}^{N-\tau}(x_i[t] - \bar{x_i})(x_j[t+\tau] - \bar{x_j})$$

The maximum lag for the cross correlation of two different signals was set to 200 milliseconds (40 data points), while the autocorrelations were calculated over all possible lag times of 1 second (200 data points). For each comparison between two different channels and as described by Kramer et al., we calculated the absolute value of the cross correlation and determined its maximum value (s_{ij}) and associated lag time (l) [14]:

$$s_{ij} = max_{\tau}|CC_{ij}[l]|$$

The Fisher transformation was then applied to each maximum cross correlation value [14, 21]:

$$s_{ij}^{F}[l] = \frac{1}{2}log(\frac{1+CC_{ij}[\tau]}{1-CC_{ij}[\tau]})$$

This transforms the maximum values so they follow a more normal distribution [21]. Similarly, the autocorrelation values were Fisher transformed across all lag points [14, 21]:

$$FCC_{ii}[\tau] = \frac{1}{2}log(\frac{1+CC_{ii}[\tau]}{1-CC_{ii}[\tau]})$$

We then estimated the variance of the cross-correlation between any two electrodes using the Fisher transformed autocorrelations and the lag at which maximum cross correlation of the two signals occurred (l) [14, 20]:

$$var(CC_{ij}[l]) = \frac{1}{n-l}\sum_{\tau=-n}^{n} FCC_{ii}[\tau]FCC_{jj}[\tau]$$

Finally, we calculated a normalized z value for the maximum cross-correlation using the variance [14]:

$$z_{ij}^{F} = \frac{s_{ij}^{F}}{(var(CC_{ij}[l]))^{1/2}}$$

The scaled z value served as a measure of the strength of the cross correlation between two electrodes for the given 1-second interval.

4. Resolving Volume Conduction and Common Average Effects

Volume conduction is the transfer of the signal from source to multiple electrode recording devices through the brain, which is recorded at the same time point [15]. This is a problem for EEG measurements as the signals from a common source may lead to coupled scalp EEG signals on the electrodes [19]. In order to account for this issue in our measurements, we removed any cross correlations between electrodes that occurred at a lag (τ) of 0. This can be an effective technique for negating the effects of volume conduction [15]. This also solves the issue of common average referencing that may artificially cause strong correlations between two channels that may have been inactive EEG [15].

5. Partial Cross Correlation

We also accounted for the possibility that the use of the common average reference resulted in artificially high cross correlation values. One solution to this issue is to implement a partial cross correlation as verification that the common average was not affecting the cross correlation. This is done by measuring the linear relationship between two signals while holding a third signal constant [19]:

$$r_{ij \cdot z} = \frac{r_{ij} - r_{iz} r_{jz}}{\sqrt{1 - r_{iz}^2}\sqrt{1 - r_{jz}^2}}$$

In this above equation, i and j represent two electrode signals, while z represents the common average reference. Partial correlation coefficient and cross correlation coefficient was calculated for each electrode comparison in a given 1-second interval. If the cross correlation coefficient was greater than the partial correlation coefficient by 0.25, then the comparison of the two electrodes at that given second was removed from analysis due to the common average reference affecting the calculations. The 0.25 threshold was determined from three different case examples that looked at all differences in electrode coefficient comparisons, and plotted in a histogram, as seen in Figure 1. Note that, in most cases, the partial correlation calculation differs from the cross correlation by less than 0.1, indicating that the reference is not causing spurious correlations. The threshold of 0.25 is meant to remove the small number of cases where the cross correlation coefficient is greatly affected by the common average reference.

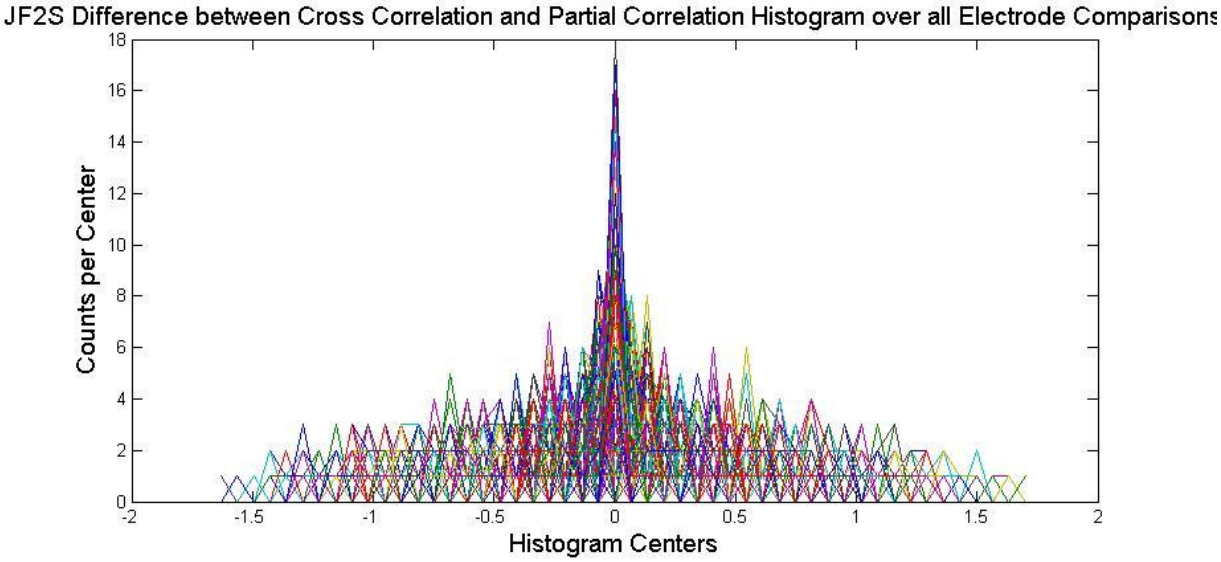

Figure 1. Difference between Cross Correlation coefficient and Partial Cross Correlation Coefficient for patient JF under the state 2S. Based on this histogram and two other subjects, a threshold for the difference was set at 0.25 to avoid any significant impacts that the common average reference may have. Each color line is a histogram of a pair of electrode comparisons difference between cross correlation coefficient and partial cross correlation coefficient.

6. Non-Parametric Permutation Testing

In order to test the significance of the scaled z value for a given electrode comparison, we implemented a non-parametric permutation test using pixel based statistics to define a threshold [19]. In comparing two electrodes for the cross correlation analysis, one electrode was of the fixed time signal and the second was of a randomly shifted time series. The random shift was ensured to have no overlap with the original time series, and all data points were shifted by a random number with any extra EEG data moved to the front of the data. Then, a random 1 second interval was taken across all electrodes. The cross correlation analysis proceeded with the equations given in the Cross Correlation Analysis section (Chapter 1, Section 3), including the correction for Volume conduction. Once the calculations were completed, the maximum cross correlation result was saved and the simulation repeated 1000 times. The maximum values were then binned via histogram, and the threshold value (Z_{thresh}) was set at the 95% maximum percentile. To be convinced that this non-parametric randomization is valid and the 95% maximum should determine the threshold value, the distribution of the maximum values were inspected, as shown for a one case scenario in Figure 2. This non-parametric randomization to determine threshold destroys any temporal connections between the two electrodes, and is meant to account for multiple comparisons [19].

Any cross correlation calculated from a one-second window of data that was above the 95% threshold was given a binary value of 1 and those that were below were given a value of 0.

$$\rho_{ij} = \begin{cases} 0 \; if \; z_{ij}^{F} < Z_{thresh} \\ 1 \; if \; z_{ij}^{F} > Z_{thresh} \end{cases}$$

With all these binary values computed, the values for a given electrode pair were averaged over the entirety of the data, which we will define as $\bar{\rho}_{ij}$. Thus, an average value of 1 for a given

electrode pair would have been consistently above the threshold in the cross correlation analysis over all one-second windows.

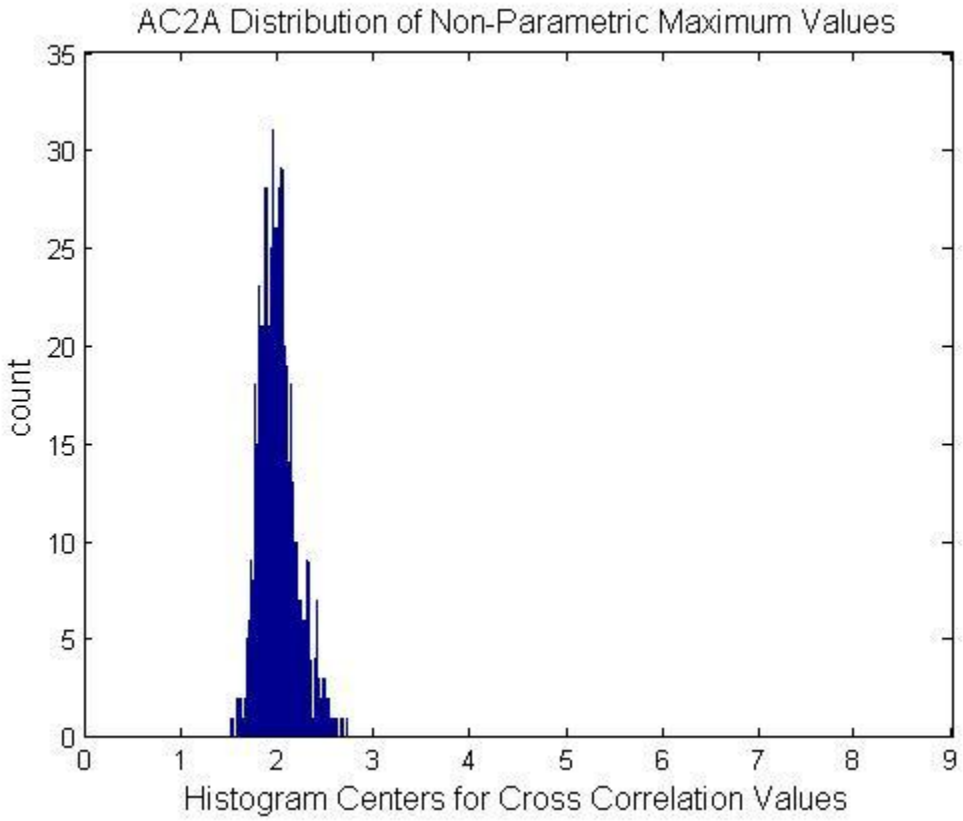

Figure 2. Patient AC under the state of 2A shows the histogram distribution of 1000 maximum values generated by the non-parametric randomization analysis. We used a 95% percentile to define the threshold for each individual patient.

7. Non-Parametric Determination of Significant Edges for Visualization

With each electrode pairing having an attributed strength, visualization of the electrode strength on a brain map is difficult. Viewing all electrode strengths would hinder the ability to understand where the strongest electrode connections are. In order to avoid the issue of displaying the weaker connections on the brain map, a non-parametric statistic was incorporated [22]. In this statistic, a determination of the 75% value of the averages (Q3), a determination of

the 25% value of the averages (Q1), and the inter-quartile range (IQR) was necessary. IQR equation is given as follows:

$$IQR = Q3 - Q1$$

With these values obtained, the non-parametric statistic defines a threshold value determined by:

$$Thresh = Q3 + 1.5 * IQR$$

This would indicate that any value above this non-parametric threshold would be considered significant. This threshold was used to visualize the stronger electrode pair connections.

8. Individual Patient Analysis of Network Stability

Network stability was calculated using the average cross correlation values for each electrode pair in each patient's state and drug condition. To display stability for the network, temporal windows ranging from 50 to 500 seconds increasing in increments of 50 seconds were created. Each group in the temporal window ($[t]$) averaged $\bar{\rho}_{ij}$ for a given pair of electrodes (ij) across all seconds defined by the temporal window. For example, in a temporal window of 50 seconds, the first group in the window would average all $\bar{\rho}_{ij}$ for all pairs of electrodes from 1 to 50 seconds. With the groups (k) defined for a given temporal window, the change, for each pair of electrodes, was calculated by subtracting the calculated average cross correlation values with the average cross correlation values in the preceding group ($k-1$). The change was then averaged over all electrode pairings to give a resulting value ($NS[t]_{\bar{k}}$). This was repeated for all groups (k) within each temporal window to display values of the network stability for the given window. If the connectivity results for each electrode pair are exactly the same in two successive windows, this total change will be zero. All average change for the group values within the temporal window were then averaged to give the overall network stability for a given temporal

window ($\overline{NS[t]}$) in a given patient, denoted by a circle in the respective Figure. The equation for a given group within the temporal window ($[t]$):

$$\overline{NS[t]} = \frac{\sum_2^{\mathrm{k}}((\sum_1^j(\sum_1^i(|\overline{CC[t]}_{ij,k} - \overline{\mathrm{CC[t]}}_{\mathrm{ij,k-1}}|)))/(i \times j)/2)}{k}$$

The overall network stability for a given group process was repeated for all temporal windows that yielded a resulting trend of means. Thus, if the network is stable over long stretches of time, then the difference will become less as the temporal window increases. However, if the networks are not stable, we would expect larger differences between successive measurements.

9. Histogram of Hypsarrhythmia and Non-Hypsarrhythmia Patients

In order to compare the groups of Hypsarrhythmia and Non-Hypsarrhythmia patients at each state of patient (A,S) and condition of the drug (1,2), a histogram plot of the average cross correlation values for each electrode pair for all patients in a group were created with bin-size increments of .005. To compare the groups statistically, a two-sample Kolmogorov-Smirnov (KS) test was calculated for each condition/state under the null hypothesis that both groups come for the same distribution [23]. The statistical test was under a MATLAB function of *kstest2* [24].

Due to many zero cross-correlation values potentially hindering the results of the null hypothesis, another histogram plot and two sample KS test was repeated with only the average cross correlations values greater than 0.

10. Electrode Distance compared to Cross Correlation Values

To determine if long range connections are much more prevalent in hypsarrhythmia patients than non-hypsarrhythmia patients, a comparison of electrode distance to cross correlation values was necessary. The distance between each pair of electrodes was calculated with the function *elec_distance*, which determined the spherical arc length of the electrode distances [25]. The distances defined were based on an adult head and we are assuming that the relative distances are the same, and thus, the units for distance we will keep as units. If we did not correct for volume conduction, the correlation with distance would follow an approximate linear relationship [19, 26]. However, since we did account for volume conduction, there is no longer a linear relationship of correlation with distance and another method of comparing distance with correlation was required [14, 19, 26]. Thus, we defined short distances on approximate distance between adjacent electrodes (S), long distances on approximate distance of electrodes opposite of the scalp (L), and all distances that were in between were grouped in middle (M). Short distance had a threshold of less than or equal to 92.06 units and long distances was defined as distances greater than or equal to 158 units. With the S, M, and L groups created, the average cross correlation values based on hypsarrhythmia and non-hypsarrhythmia were grouped. These groups were then compared via an n-way analysis of variance (ANOVAN) with the MATLAB function *anovan* [27] and group were further classified with function *multcompare* [28, 29], which accounted for multiple comparisons. The null hypothesis for comparing the groups from *multcompare* is that there is no difference in the means of the interaction of the groups.

11. Statistics Comparing Hypsarrhythmia and Non-Hypsarrhythmia Patients

Further statistics were calculated to compare the hypsarrhythmia and non-hypsarrhythmia patient's $\bar{\rho}_{ij}$ based on states and conditions. These statistics were compared in two ways. A group based statistic using an n-way analysis of variance (ANOVAN) with the MATLAB function *anovan* [27] and were further compared with the function *multcompare* [28, 29], which accounted for multiple comparisons. The null hypothesis for comparing the groups from *multcompare* is that there is no difference in the means of the interaction of the groups. To compare electrode cross correlation values directly between groups, a paired t-test was conducted on only patients that had pre- and post- treatment EEG readings. Null hypothesis for the paired t-test is that the difference in means of the groups is zero. The paired t-test was completed with the MATLAB function *ttest* [30].

Another paired t-test was incorporated to view the differences between hypsarrhythmia responders before and after treatment, hypsarrhythmia non-responders before and after treatment, non-hypsarrhythmia responders before and after treatment. Non-hypsarrhythmia non-responders could not be evaluated due to zero sample size. Null hypothesis for paired t-tests are that the means are equal.

Chapter 2: Results

1. Visualization of Connectivity Results

With the $\bar{\rho}_{ij}$ computed, a heat map of the overall connectivity measures, as defined in Chapter 1 Section 6, on a patient level is displayed. Each heat map is set on connectivity limits from 0 (blue) to 0.3 (red). The cross between a row to a column is a representation of the connectivity between two electrodes. In the heat map, the diagonal from top left to the bottom right are the auto-correlations. For the figures, Figure 3 and Figure 4, each displays the two patients of hypsarrhythmia and non-hypsarrhythmia patients, respectively. The rows for each figure are of the states/conditions of 1A, 1S, 2A, and 2S, respectively. Other patients' heat maps can be seen in Supplementary Figure 1 and Supplementary Figure 2.

With the connectivity results, a non-parametric determination of significant edges was calculated, as seen in Section Non-parametric Permutation Testing (Chapter 1, Section 7). These results are meant to act as a visual representation of the strongest connectivity in each state of the patient. The figures, Figure 5 and Figure 6, are representative of the two patients of hypsarrhythmia and non-hypsarrhythmia, respectively. Each figure contains individual brain maps with the rows representing the states/conditions of 1A, 1S, 2A, and 2S, respectively. Each diagram of the patient displays a visual electrode map of the brain, with the anterior region of the brain on the right side of the diagram. Furthermore, each line connecting two electrodes is a representation of a significant edge between the two electrodes. For a given diagram, if an electrode marker is removed, it is meant to represent a noisy electrode that was deemed unfit for calculations. Other patients' visual connectivity can be seen in Supplementary Figure 3 and Supplementary Figure 4.

In viewing each figure, all patients have unique connectivity results relative to other patients within the same state. Furthermore, it can be noted that there are generally more significant connections before treatment and more connections during sleep states than awake, which may be attributed to lower correlation dimension and lower entropy [17,18]. There are some similarities in that there are strong connectivity in the frontal regions (Fp1 and Fp2) and along F8, T8, F7, and T7 which may be attributed to artifacts, such as eye movements and blinks.

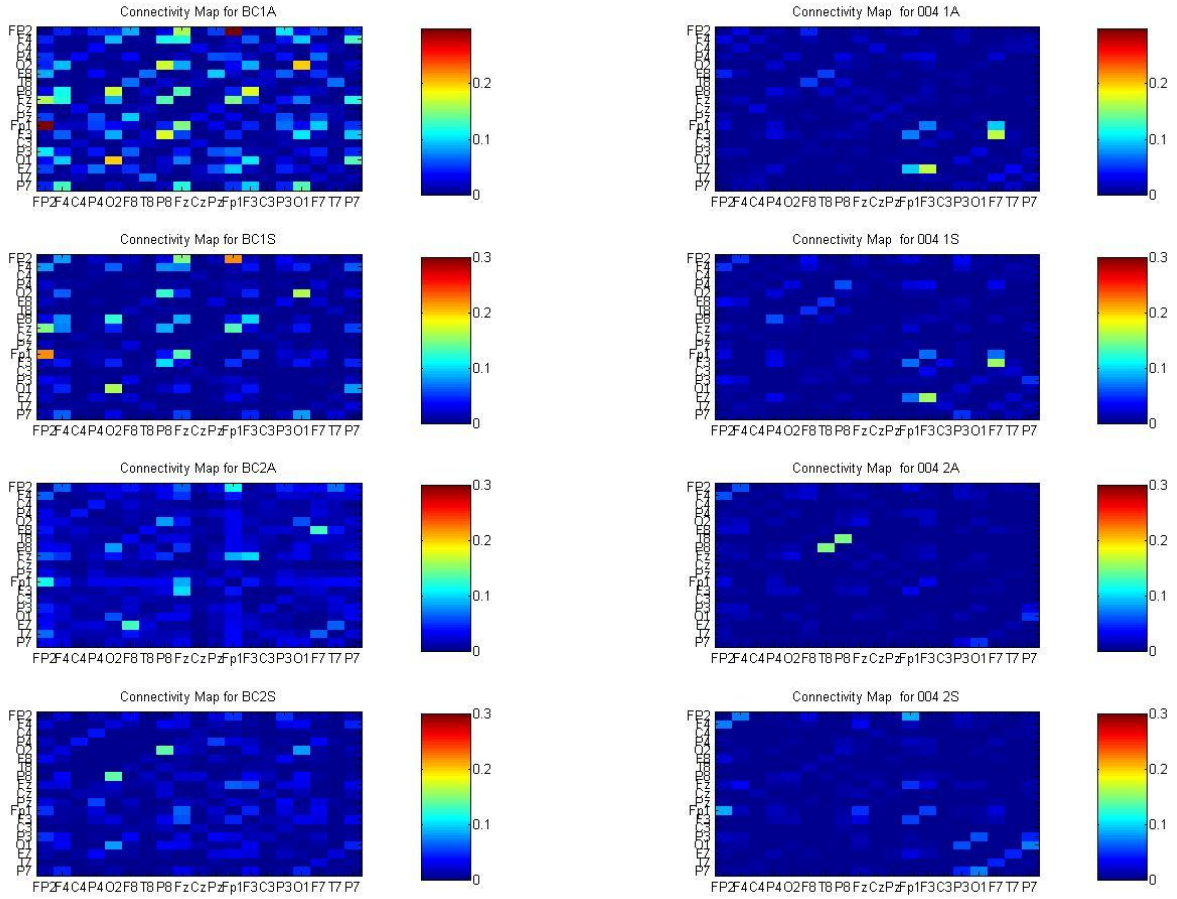

Figure 3. A connectivity map of two Hypsarrhythmia patients, in which color of blue (0) to red (.3) represents the strength of the average connectivity between two electrodes. The x and y axis are the electrodes being compared. There are 4 rows of heat maps, which represent the different states/conditions of where it is 1A, 1S, 2A, and 2S, respectively.

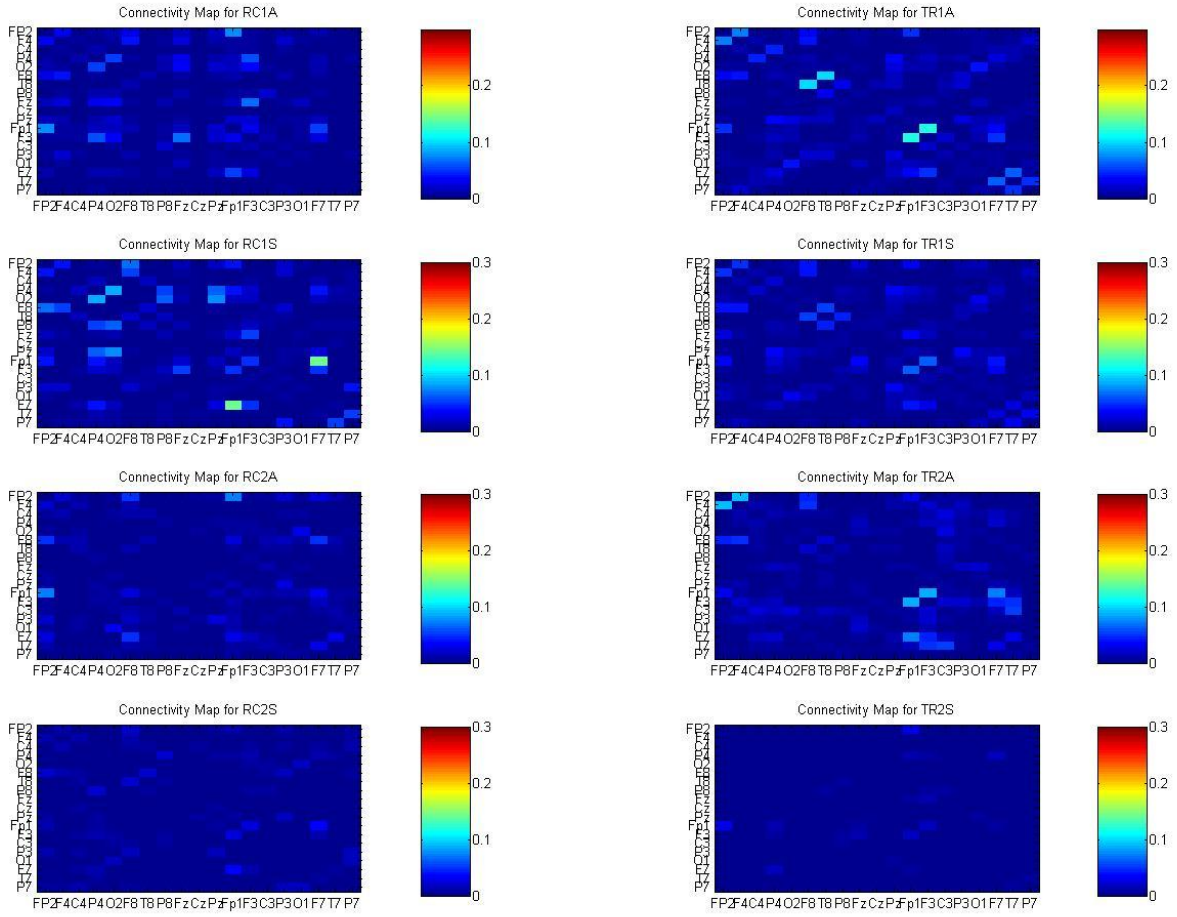

Figure 4. A connectivity map of two Non-Hypsarrhythmia patients, in which color of blue (0) to red (.3) represents the strength of the average connectivity between two electrodes. The x and y axis are the electrodes being compared. There are 4 rows of heat maps, which represent the different states/conditions of where it is 1A, 1S, 2A, and 2S, respectively.

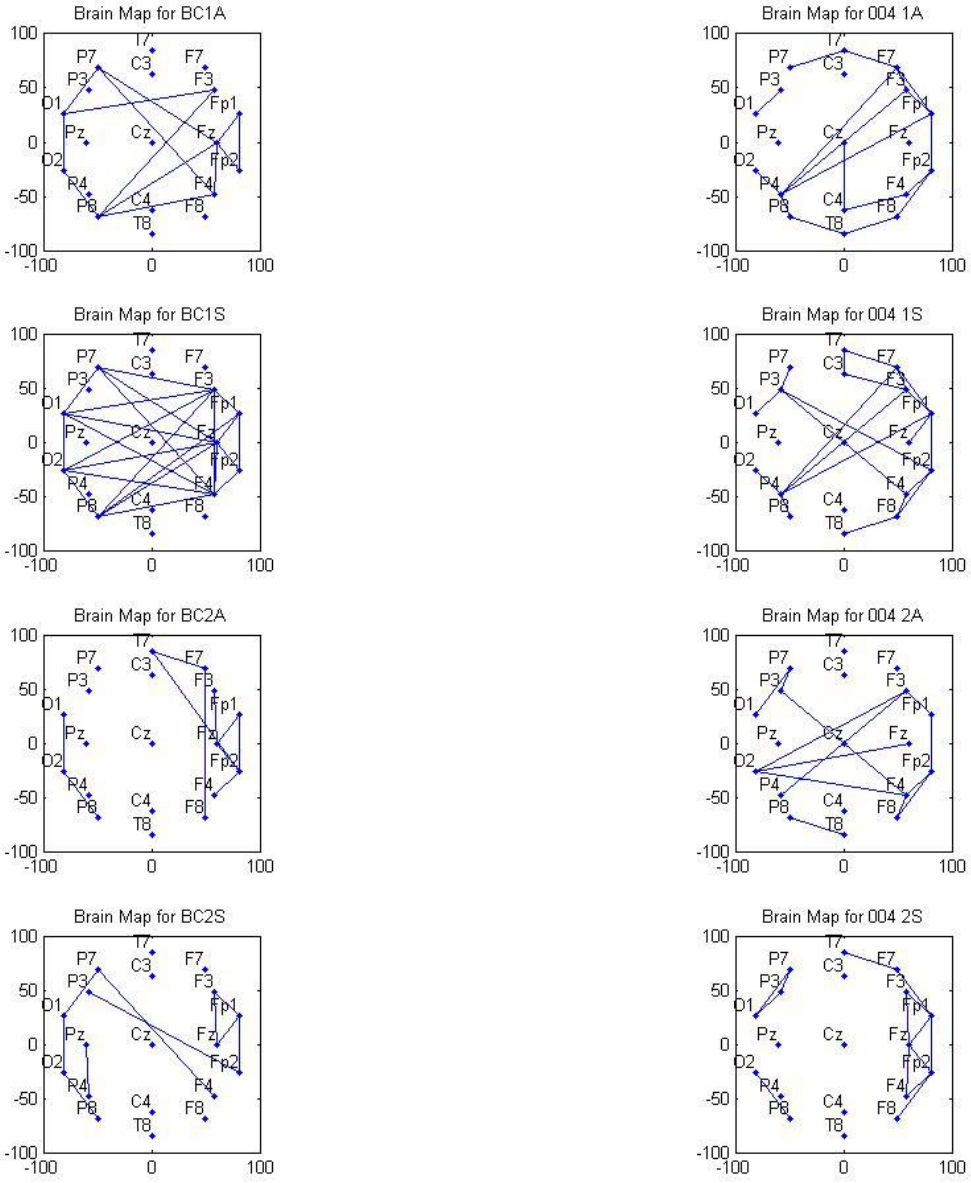

Figure 5. Brain map of two Hypsarrhythmia patients' connectivity. Each line, for the patient data, is a representation of a strong connection (greater than the 1.5*IQR+Q3 threshold) for the given patient. There are 4 rows of heat maps, which represent the different states/conditions of where it is 1A, 1S, 2A, and 2S, respectively. This visual representation displays how unique each individual's connectivity is with only a few commonalities.

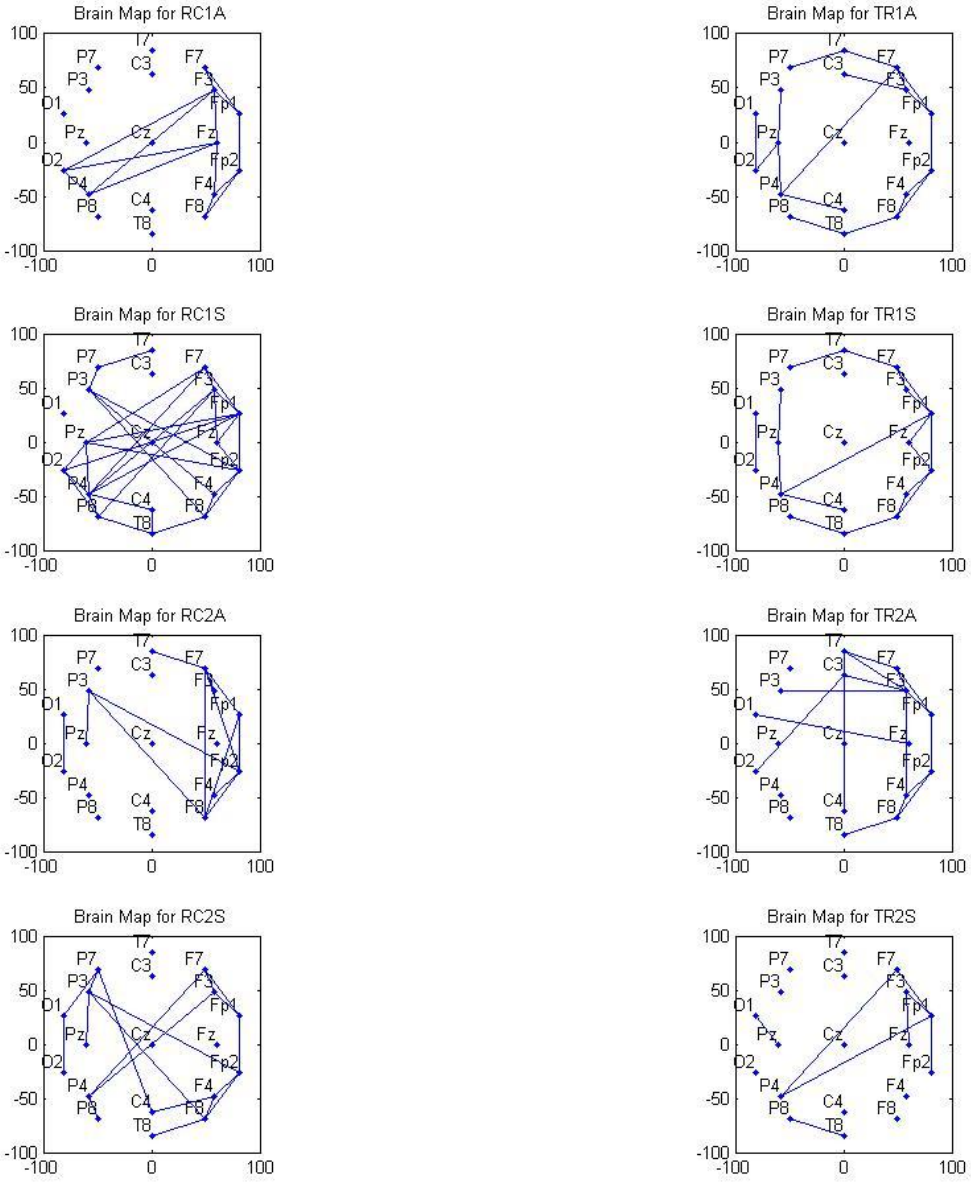

Figure 6. Brain map of Non-Hypsarrhythmia patients' connectivity. Each line, for the patient data, is a representation of a strong connection (greater than the 1.5*IQR+Q3 threshold) for the given patient. There are 4 rows of heat maps, which represent the different states/conditions of where it is 1A, 1S, 2A, and 2S, respectively. This visual representation displays how unique each individual's connectivity is with only a few commonalities.

2. Stability of Connectivity is Shown with Increased Temporal Window

To view how stable a patient's connectivity is, we measured the mean average change between two groups within each temporal window. Figure 7, Figure 8, Figure 9, and Figure 10 are representations of state 1A, 1S, 2A, and 2S, respectively. Given that an interval will be defined as the average of all electrode pairs, the circle represents the mean of average change of each patient for the given temporal window. Red represents a hypsarrhythmia patient and blue represents a non-hypsarrhythmia patient. In order to clearly view average change for each patient within a figure for a given group temporal window, all patients were offset from each other between the beginning of the current interval to the beginning of the following interval. For example, for groups in the temporal window of 50 seconds, one patient would be displayed at exactly on 50 second, the second patient is on 53.33 second, the next patient is on 56.66, and this continues until 96.66 seconds. All patients between 50 seconds to 96.66 seconds represent only the 50 second temporal window interval size.

Figure 7, Figure 8, Figure 9, and Figure 10 all see a decrease in average change as the temporal window increases. Thus, a more stable network can be seen across all patients in all sizes/groups as temporal window increases. In the state of 2S, a lower average change can be noted relative to other states/conditions. For all states/conditions, there is little noticeable difference between hypsarrhythmia and non-hypsarrhythmia patients in network stability.

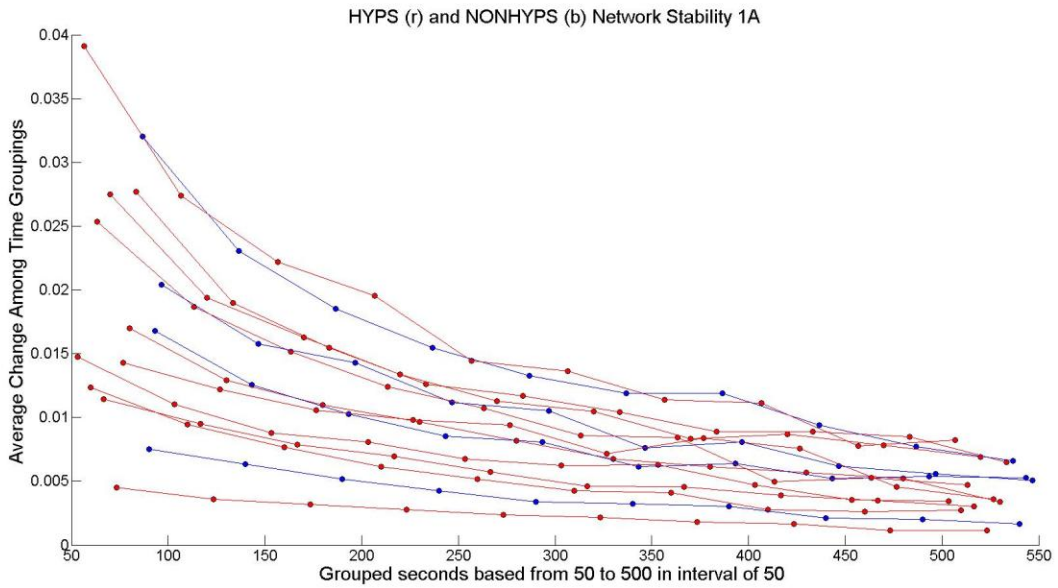

Figure 7. Average change of all patients in state 1A. Red line represents hypsarrhythmia patients and blue line represents non-hypsarrhythmia patients. The circle represents the mean of all the average changes for a given patient. Temporal windows were generated from 50 to 500 seconds with increasing intervals of 50 seconds. All patients within the 50 interval group are displayed in the same temporal window. A decrease in average change can be seen with increasing temporal windows, indicating that the connectivity networks are stable.

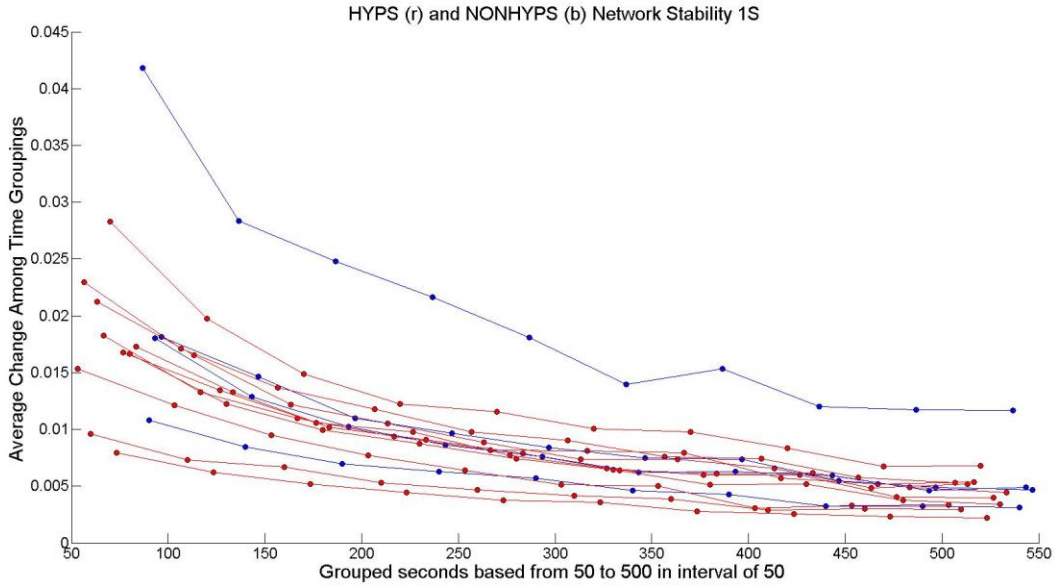

Figure 8. Average change of all patients in state 1S. For description on each symbol and color see Figure 7. A decrease in average change can be seen with increasing temporal windows, indicating that the connectivity networks are stable.

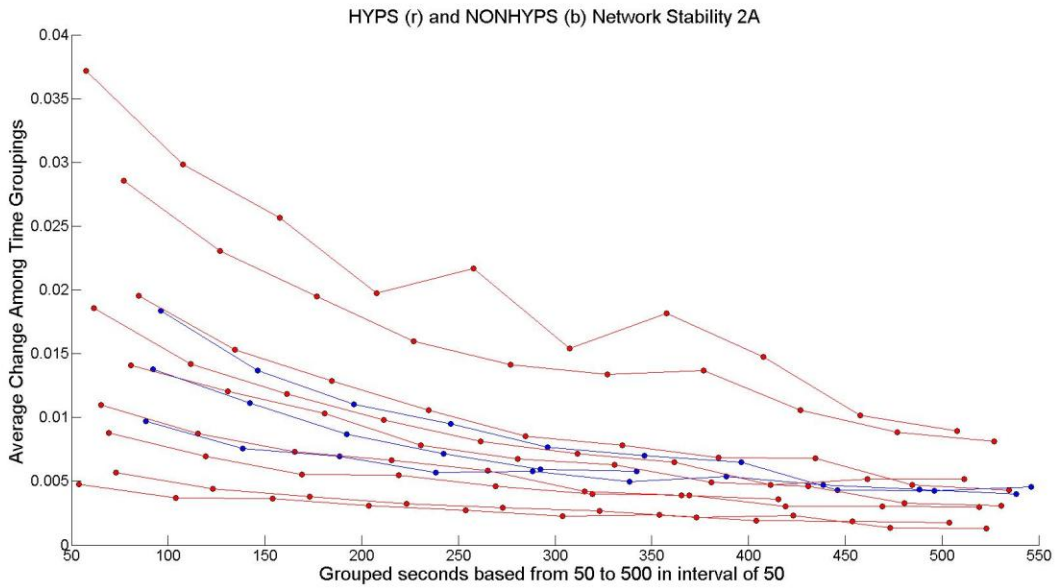

Figure 9. Average change of all patients in state 2A. For description on each symbol and color see Figure 7. A decrease in average change can be seen with increasing temporal windows, indicating that the connectivity networks are stable.

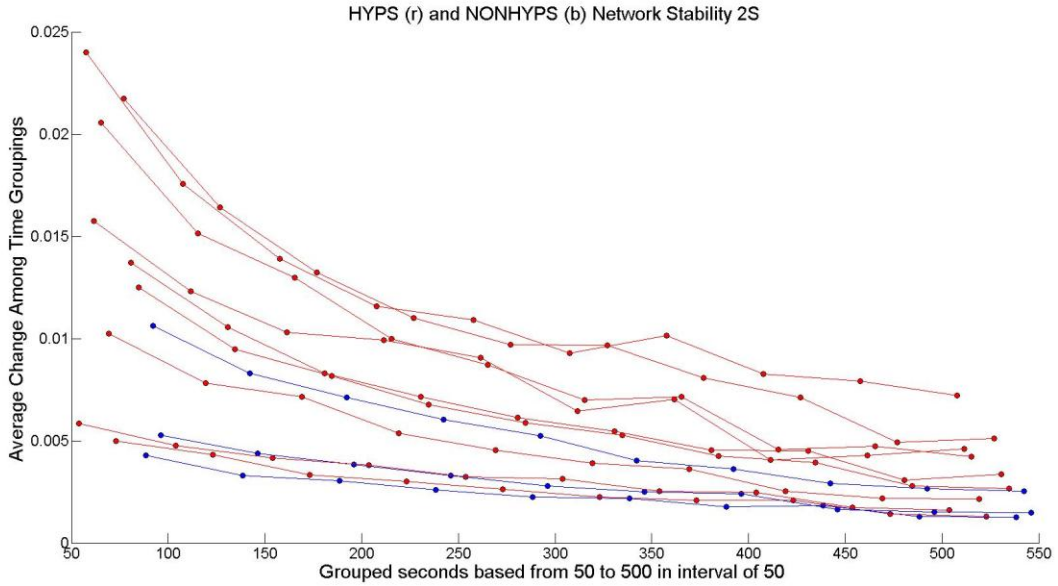

Figure 10. Average change of all patients in state 2S. For description on each symbol and color see Figure 7. A decrease in average change can be seen with increasing temporal windows, indicating that the connectivity networks are stable.

3. Distributions of Hypsarrhythmia and Non-Hypsarrhythmia Patients Show Significance

The distribution of $\bar{\rho}_{ij}$, as defined in Chapter 1 Section 6, of hypsarrhythmia and non-hypsarrhythmia can be seen in Figure 11 and Figure 12. Each row shows the condition/state of patients in 1A, 1S, 2A, and 2S. The first column represents all the hypsarrhythmia patients of that condition/state in red and the second column is of all the non-hypsarrhythmia patients of that condition/state in blue. Because the zero $\bar{\rho}_{ij}$ were affecting the viewability of the distributions, a representation of the histogram plots are displayed without the zero $\bar{\rho}_{ij}$ (in Figure 11).

To calculate if the two distributions are different, a two-sample KS-test was implemented and the results are in Table 2. The null hypothesis for the KS-test is that the two samples are coming from the same distribution. The KS-test, as seen in Table 2, is calculated on the distributions for each state both with and without zero $\bar{\rho}_{ij}$. From these results, we can see over all four different states/conditions that the p-value is less than .05. This means that the distributions of hypsarrhythmia and non-hypsarrhythmia patients are from different distributions, and are unrelated. It is also noted that zero $\bar{\rho}_{ij}$ had no effect on the KS-test.

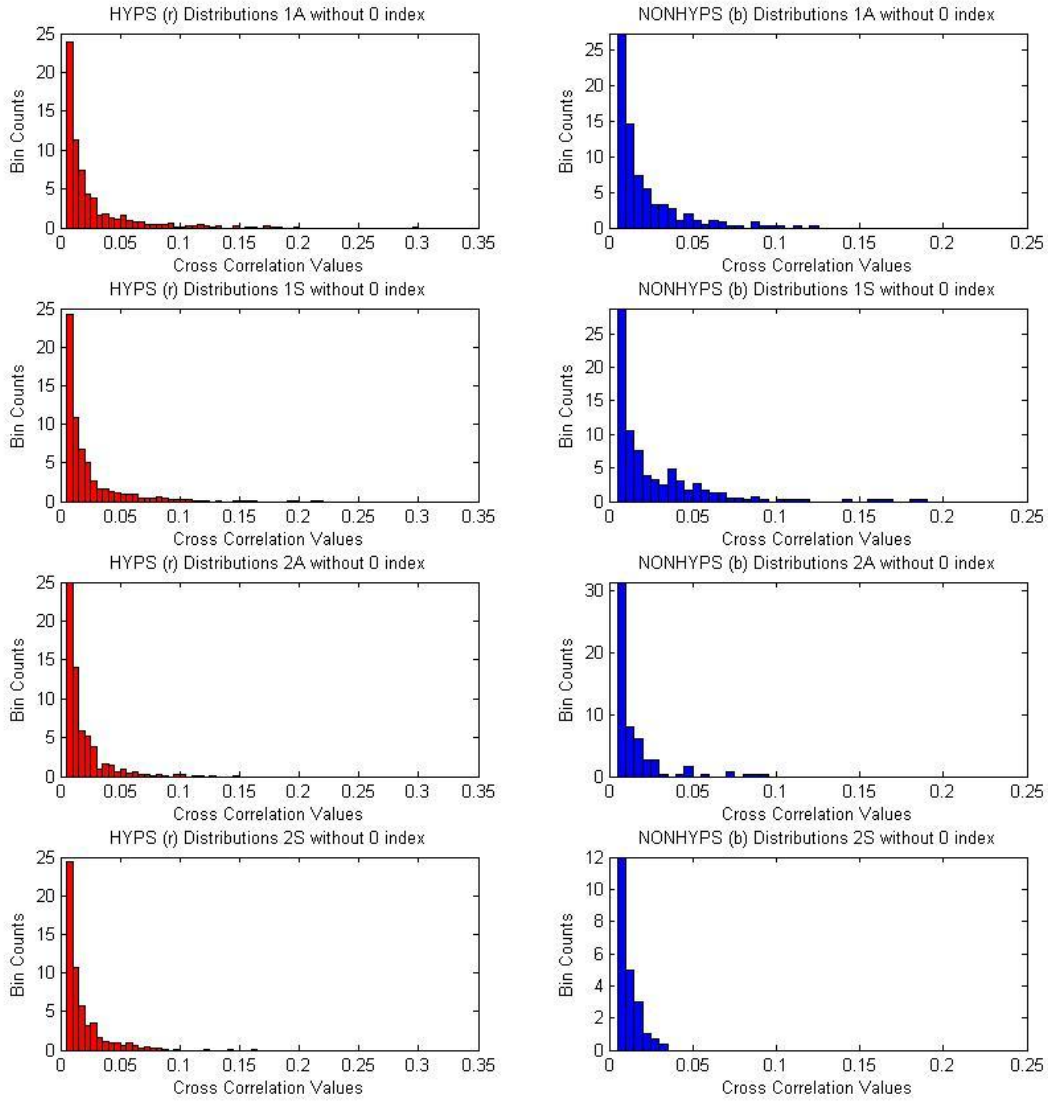

Figure 11. Histogram plot depicting the $\bar{\rho}_{ij}$ of all patients and electrode comparisons within each category, but does not include zero $\bar{\rho}_{ij}$. Each row is a representation of state, which is 1A, 1S, 2A, and 2S, respectively. The left column (red) is the histogram of hypsarrhythmia patients and the second column (blue) is the histogram of non-hypsarrhythmia patients. In this figure, the distributions of the two types of patients can be seen more clearly to be different with Hypsarrhythmia patient having longer tails than non-hypsarrhythmia patients.

KS-TEST of Hypsarrhythmia versus Non-Hypsarrhythmia				
	1A	1S	2A	2S
with Zero $\bar{\rho}_{ij}$ Included	**1.74E-02**	**1.83E-08**	**1.72E-06**	**1.24E-17**
without Zero $\bar{\rho}_{ij}$ Included	**5.80E-03**	**1.07E-06**	**2.80E-04**	**5.91E-14**

Table 2. Results of the two sample KS-Test on the distributions of the Connectivity Values. Null hypothesis of this test is that the distributions of both samples come from the same distribution. Any p-values less than .05 are bolded. The results show that regardless of including zero $\bar{\rho}_{ij}$, the distributions over all states/conditions come from different distributions (having p-values less than .05).

4. Electrode Distance to Average Connectivity shows Higher Connectivity Values in Hypsarrhythmia Patients

A scatter plot of average connectivity in hypsarrhythmia and non-hypsarrhythmia patients over distance displays the differences between short, medium, and long distances. We are able to view the $\bar{\rho}_{ij}$ over distance between hypsarrhythmia (red) and non-hypsarrhythmia patients (blue) in the Figure 12 for 1A, Figure 13 for 1S, Figure 14 for 2A, and Figure 15 for 2S. The distances defined were based on an adult head and we are assuming that the relative distances are the same, and thus, the units for distance we will keep as units.

With these scatter plot figures, we see that hypsarrhythmia patients have higher $\bar{\rho}_{ij}$ values over all distances, except in the case of 1S. An intriguing point to notice is that hypsarrhythmia connectivity is stronger post-treatment than pre-treatment, where we may have suspected the connectivity strength to be similar in post-treatment. There is also a decrease in average connectivity as the distance increases, except for long range distances that increase in connectivity. Furthermore, there appears to be many connectivity values that are below .05, which may be due to many pairs of electrodes having little connectivity in all patients.

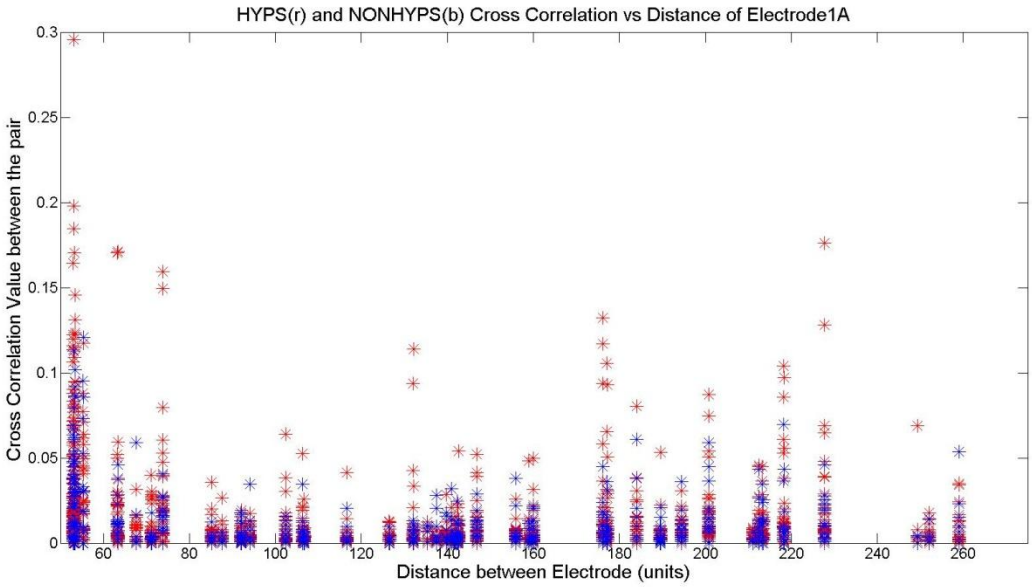

Figure 12. Scatter plot of $\bar{\rho}_{ij}$ relative to distance for condition/state 1A. Hypsarrhythmia patients are in red and non-hypsarrhythmia patients are in blue. From 1A, it can be noted that hypsarrhythmia patients have much higher connectivity values than non-hypsarrhythmia, and that there are many connectivity values that are near 0.

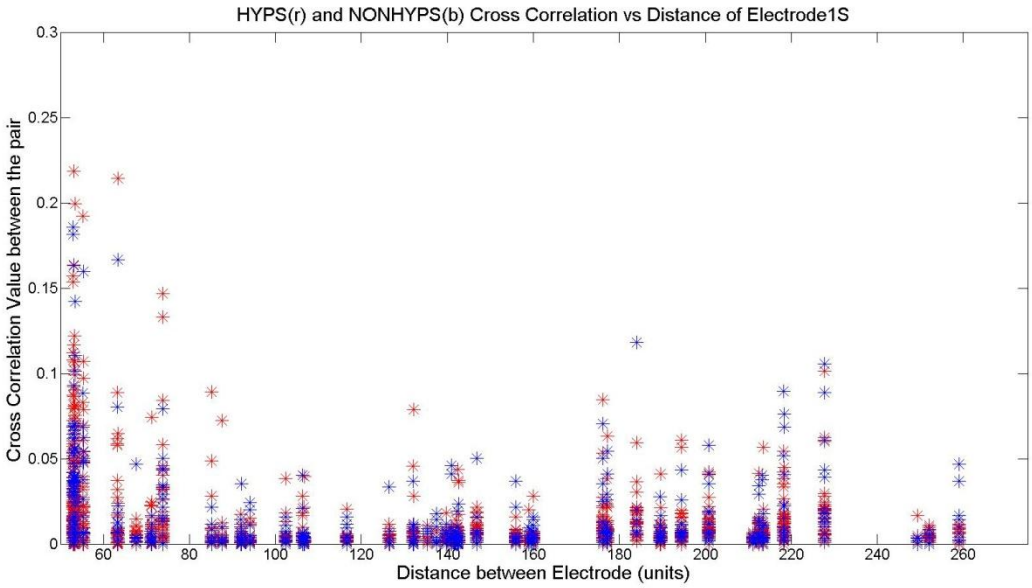

Figure 13. Scatter plot of $\bar{\rho}_{ij}$ relative to distance for condition/state 1S. Hypsarrhythmia patients are in red and non-hypsarrhythmia patients are in blue. In 1S, it can be noted that hypsarrhythmia patients and non-hypsarrhythmia have the same spread of connectivity, and that there are many connectivity values near 0.

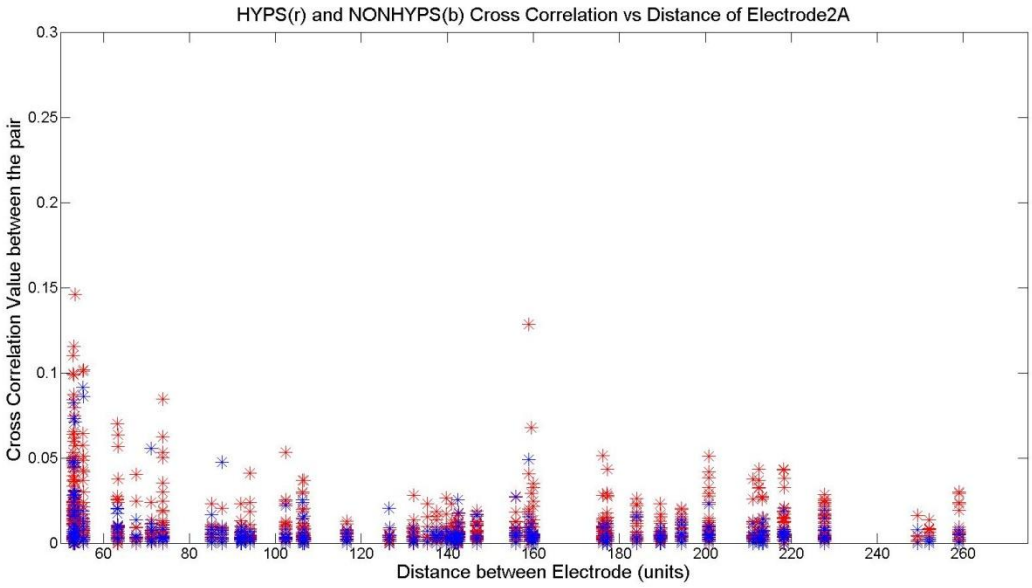

Figure 14. Scatter plot of $\bar{\rho}_{ij}$ relative to distance for condition/state 2A. Hypsarrhythmia patients are in red and non-hypsarrhythmia patients are in blue. In this figure, hypsarrhythmia patients have much higher connectivity values than non-hypsarrhythmia, and that there are many connectivity values that are near 0.

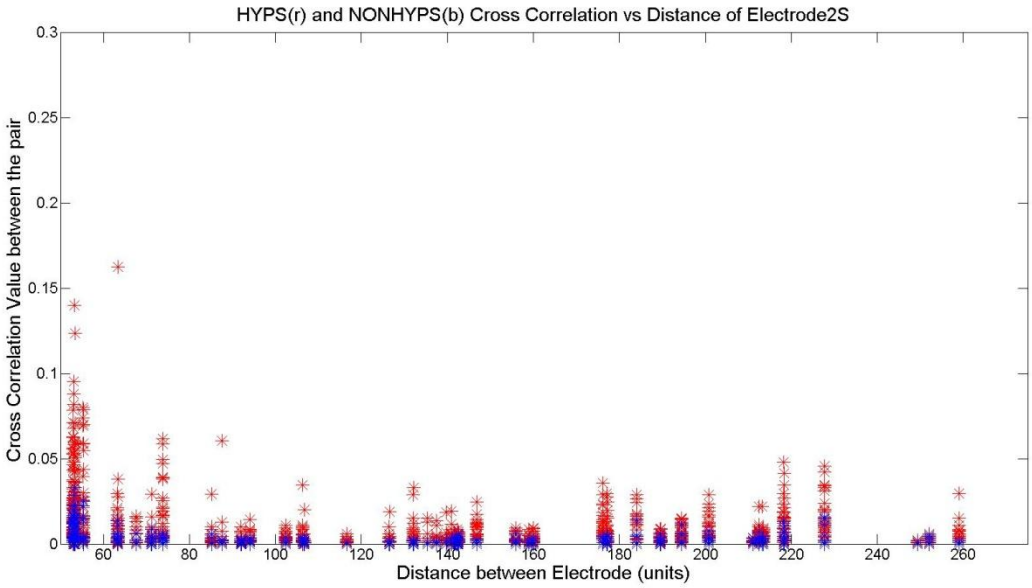

Figure 15. Scatter plot of $\bar{\rho}_{ij}$ relative to distance for condition/state 2S. Hypsarrhythmia patients are in red and non-hypsarrhythmia patients are in blue. The 2S state has hypsarrhythmia patients with much higher connectivity values over all distances than non-hypsarrhythmia, and that there are many connectivity values that are near 0.

5. Statistical Results on Comparison of Groups of Patients

The ANOVAN compares unequal groups of hypsarrhythmia's and non-hypsarrhythmia's $\bar{\rho}_{ij}$ values based on distance between the different states/conditions. Table 3 shows the results of comparing groups of distances within each state. In hypsarrhythmia patients, there are statistical differences in all states when comparing short, medium, long distances, which is consistent with the results seen in Figures 12-15. These results show that connectivity in short distances is higher than connectivity in medium and long distances, and connectivity in long distances is higher than medium distances. Whereas, for non-hypsarrhythmia patients, there is a statistical connectivity increase from short to medium distances in all states, and in short to long distances, except in the 2S state. It was also noted for 1S that connectivity is significantly larger in long distances than in medium. In comparing the connectivity and distances between hypsarrhythmia and non-hypsarrhythmia, hypsarrhythmia patients have significantly higher connectivity in sleep states for long distances pre- and post- treatment and in post-treatment for short distance.

A paired t-test displays the paired comparison between patients in the various states/conditions of hypsarrhythmia or non-hypsarrhythmia patients by comparing the same pair of electrodes directly in the different conditions. This allows for more patient and electrode specific changes in connectivity, unlike ANOVAN, which compares the full distribution of patients. Table 4 shows the statistical tests for the grouping of hypsarrhythmia and non-hypsarrhythmia through ANOVAN and paired t-test. The paired t-test shows that hypsarrhythmia groups are significant when comparing all states, and even more statistically significant between pre- and post- treatment. Non-hypsarrhythmia patients are significant post-treatment groups and in comparing the sleep states pre- to post- treatment. ANOVAN displays the same results for non-hypsarrhythmia for significance and shows that there is higher connectivity pre-treatment

than post-treatment in sleep states and higher connectivity in the awake sate than sleep state post-treatment. In hypsarrhythmia, there is only significantly higher connectivity pre-treatment than post-treatment for the same state. Additionally, comparing overall connectivity between hypsarrhythmia and non-hypsarrhythmia over the same state shows higher significant connectivity for hypsarrhythmia than non-hypsarrhythmia in 1A, 1S, and 2A.

Some patients did not respond to treatment, which may have hypsarrhythmia EEG patterns that may affect the results, so we divided the patients into those who responded and those that did not. Paired t-test is also conducted on the hypsarrhythmia responder's pre- versus post- treatment, hypsarrhythmia non-responder's pre- versus post- treatment, and non-hypsarrhythmia responder's pre- versus post- treatment. This t-test is meant to validate whether treatments are affecting connectivity through a direct t-test comparison. Thus, the t-test is calculated between 1A to 2A and between 1S to 2S, which are displayed in Table 5. From these results we are able to conclude that hypsarrhythmia responders and non-responders are statistically significant between pre- and post- treatment. However, non-hypsarrhythmia responders are only statistically significant in the sleep state pre- versus post- treatment.

ANOVAN Results for cross correlation versus Distance [Mean1 - Mean2 (p-Value)]				
Hypsarrhythmia (H)	1A	1S	2A	2S
S-M	.0214-.0042 **(2.06E-08)**	.0202-.0031 **(2.06E-08)**	.0132-.0038 **(2.06E-08)**	.0141-.0024 **(2.06E-08)**
M-L	.0042-.0103 **(2.59E-06)**	.0031-.0079 **(2.43E-04)**	.0038-.0073 **(7.5260E-05)**	.0024-.0059 **(2.34E-06)**
S-L	.0214-.0103 **(2.06E-08)**	.0202-.0079 **(2.06E-08)**	.0132-.0073 **(2.0676E-08)**	.0141-.0059 **(2.06E-08)**
Non-hypsarrhythmia (NH)				
S-M	.0173-.0044 **(2.10E-08)**	.0247-.0044 **(2.06E-08)**	.0110-.0039 **(3.06E-06)**	.0048-.0007 **(1.02E-02)**
M-L	.0044-.0088 (1.56E-01)	.0044-.0123 **(1.33E-04)**	.0039-.0044 (9.98E-01)	.0007-.0021 (8.36E-01)
S-L	.0173-.0088 **(3.33E-04)**	.0247-.0123 **(2.27E-08)**	.0110-.0044 **(5.28E-05)**	.0048-.0021 (2.66E-01)
Hypsarrhythmia (H) to non-hypsarrhythmia (NH)				
H S-NH S	.0214-.0173 (1.73E-01)	.0202-.0247 (8.14E-02)	.0132-.0110 (4.31E-01)	.0141-.0048 **(2.06E-08)**
H M- NH M	.0042-.0044 (1.00E+00)	.0031-.0044 (9.36E-01)	.0038-.0039 (1.00E+00)	.0024-.0007 (4.28E-01)
H L- NH L	.0103-.0088 (9.40E-01)	.0079-.0123 **(5.00E-02)**	.0073-.0044 (1.03E-01)	.0059-.0021 **(1.40E-03)**

Table 3. ANOVAN statistical results are shown in this table that compares the distances to cross-connectivity groups. MULTCOMPARE function on MATLAB is used to account for multiple comparisons. In this table, S stands for Short Distance (less than 92.06 u), L stands for Long distances (greater than 158 u), M stands for Medium distance (between 92.06 u and 158 u), H stands for hypsarrhythmia, and NH stands for non-hypsarrhythmia. The mean values of the groups are in the format of the label. For example, for the label S-M, the mean of the short group is before the dash and the mean of the medium group is after the dash. All p-values, in parenthesis, less than .05 are bolded, which means that the null hypothesis fails and the comparison between the groups warrant differences.

ANOVAN [Mean1 - Mean2 (p-Value)]		Paired T-test
Hypsarrhythmia (H)		
1A-1S	.0116-.0101 (2.41E-01)	**3.49E-05**
2A-2S	.0076-.0068 (9.24E-01)	**1.09E-02**
1A-2A	.0116-.0076 **(5.98E-08)**	**9.19E-15**
1S-2S	.0101-.0068 **(6.56E-10)**	**9.12E-15**
Non-Hypsarrhythmia (NH)		
1A-1S	.0068-.0075 (9.93E-01)	1.22E-01
2A-2S	.0060-.0023 **(5.80E-03)**	**7.73E-17**
1A-2A	.0068-.0060 (9.53E-01)	1.17E-01
1S-2S	.0075-.0023 **(7.01E-07)**	**6.84E-21**
Hypsarrhythmia to Non-Hypsarrhythmia		
H 1A-NH 1A	.0116-.0068 **(7.51E-08)**	
H 1S-NH 1S	.0101-.0075 **(1.01E-02)**	
H 2A- NH 2A	.0076-.0060 (3.35E-01)	
H 2S- NH 2S	.0068-.0023 **(1.86E-07)**	

Table 4. In this table, group comparisons of hypsarrhythmia and non-hypsarrhythmia patients are statistically compared among states/conditions. ANOVAN results are on the left side of column. Paired t-tests statistical test are calculated on right side of column. The mean values of the groups are in the format of the label. All p-value that are less than .05 are bolded because they signify the rejection of the null hypothesis.

Paired T-test	
Hypsarrhythmia Responders	
1A-2A	**5.4535E-12**
1S-2S	**2.8197E-11**
Hypsarrhythmia Non-Responders	
1A-2A	**2.7988E-04**
1S-2S	**8.3572E-06**
Non-Hypsarrhythmia Responders	
1A-2A	1.1780E-01
1S-2S	**6.8470E-21**

Table 5. Paired T-test is calculated between hypsarrhythmia responder's pre- versus post-treatment and hypsarrhythmia non-responder's pre- versus post- treatment. All p-value that are less than .05 are bolded because they signify the rejection of the null hypothesis. In these results, hypsarrhythmia responders and non-responders are statistically significant pre- versus post-treatment. Non-hypsarrhythmia responders are only statistically significant in the sleep state pre-versus post- treatment.

Chapter 3: Discussion

1. Connectivity Analysis Reveals Unique Networks across Subjects

In visualizing brain maps and heat maps of connectivity in hypsarrhythmia and non-hypsarrhythmia patients (Figure 3-6, Supplementary Figure 1-4), it can be seen that each patient, regardless of hypsarrhythmia or non-hypsarrhythmia, has unique connectivity. Chu et al. conducted a similar connectivity analysis on healthy patients, and through all states that were measured, all patients were seen to be unique as well [15]. Similar to Chu et al.'s findings, although there are some similar features between patients, most features are too unique to have conclusive evidence among the patients. However, there is also a noticeable strong connectivity primarily in the frontal brain (Fp1 and Fp2), and along F8, T8, F7, T7, O1, and O2. We believe this may be due to the artifacts, including movement, muscle, eye movements, or eyeblinks. Our analysis currently does not account for these artifacts due to the time consuming detection but is being considered for future methodologies. Although the artifacts exist, they are affecting the each group of patients proportionally, as we can note that both hypsarrhythmia and non-hypsarrhythmia have the same characteristic artifacts and both awake and sleep state patients contain eye-movements.

Furthermore, it can be noted that there are generally more significant connections before treatment and more connections during sleep states than awake. These results can be compared to previous research that has shown high connectivity in sleep and epileptic states, which are related to lower entropy and correlation dimension. Also, these results can be compared to previous research that has shown low connectivity in awake states, which are related to higher entropy and dimensionality [16, 17, 18].

2. Network Stability More Stable with Increasing Temporal Window Size

To discern each networks's stability, an approach of average change in overall connectivity values is calculated. Due to the disorganization EEG nature of hypsarrhythmia, we would expect that the network stability may not be prevalent. Yet in this approaches, this result shows that more stability is achieved with increasing temporal windows for both non-hypsarrhythmia and hypsarrhythmia patients. If stability is defined as an average change less than .01 for a majority of patients, the stability in state 1A begins at 400 seconds; 1S begins at 300 seconds; 2A at 300 seconds; and 2S at 200 seconds. Chu et al. had conducted a similar network analysis but on the top 5% strongest connections and found stability at approximately 200 seconds [15]. Although our results display stability at higher epoch seconds than Chu et al., the results show that network stability exists over all patients in all states through the process of average change. The increase in epoch seconds from our results could have been due to calculating the stability over all electrode pairings rather than the strongest 5% connectivity. An interesting notion from these Figures are that there were little differences in stability between hypsarrhythmia and non-hypsarrhythmia patients through the states, even though we may have expected that hypsarrhythmia would be less stable due to the disorganization of its EEG.

4. Statistical Analysis on Distance Displays Significance for Long Range Connections

To determine if long range connections are prevalent in hypsarrhythmia patients relative to non-hypsarrhythmia patients, ANOVA statistics are calculated on both the groups based on short, medium, and long distances. The short distance was determined as one electrode distance away, long distance was determined as more than two electrode distance away, and medium distance was in between short and long. Results of the analysis show that there is statistically higher connectivity in short distances than medium and long distances, and higher connectivity

in long distance than medium distances among all states/conditions for hypsarrhythmia patients (Table 3). Viewing the Figures (Figure 12-15), the means of connectivity from largest to smallest is short, long, and medium distances. This would indicate, with the statistics and means of connectivity, the long range connections are prevalent in hypsarrhythmia patients. Analysis of non-hypsarrhythmia patients, there is statistical increase from short to medium distances over all states/conditions. There is further statistical increase in connectivity for state 1S for long to medium distances, and significant increase in connectivity for states 1A, 1S, and 2A between short to long distances (Table 3). 2S between short and long distance may not be significant due to the effects of the treatment affecting the means. The medium to long distance, which is not significant in 1A, 2A, and 2S, does not indicate much about the long distance connectivity.

Comparing hypsarrhythmia and non-hypsarrhythmia patients based on distance, only the short distance in 2S and long distance in 1S and 2S show a significant increase for hypsarrhythmia patients (Table 3). From these results, we can determine that sleep state is more useful in comparing differences between the two patient groups, which may be due to lower entropy [17, 18], and a statistical difference can be seen post-treatment in short and long distances. Furthermore, we can note that long distances are statistically different in the sleep state pre-treatment, which leads to believe that there is a noticeable difference in long range connections between the groups.

5. Analysis on Hypsarrhythmia and Non-Hypsarrhythmia Patients

One comparison between the groups of hypsarrhythmia and non-hypsarrhythmia is to calculate the distribution of connectivity values. These calculations are done by KS-test, and it is calculated that in all states/conditions, the distributions of hypsarrhythmia and non-hypsarrhythmia patients are significantly different (Table 2). From these results, we can

conclusively determine that is there a difference between hypsarrhythmia and non-hypsarrhythmia patients based on distributions of connectivity alone.

Hypsarrhythmia and non-hypsarrhythmia patients are also statistically calculated to compare the differences between states/conditions through ANOVAN. If a comparison had the same sample size, that comparison was also statistically calculated through a paired t-test to analyze a direct comparison between same electrode pairing. Within the hypsarrhythmia patients, ANOVAN results shows statistical increase in connectivity in comparing pre- versus post-conditions, whereas paired t-test shows statistical significance in comparing pre- versus post- and between awake and sleep states. These results indicate that the treatment may be effective such that there is a difference between pre- versus post- conditions. Within non-hypsarrhythmia patients, statistical increase for ANOVAN and statistical significance for paired t-test are only displayed in post awake and sleep state and in comparing pre- versus post- sleep conditions. Further analysis was conducted to compare hypsarrhythmia and non-hypsarrhythmia for each condition/state, which shows statistical increase in all states/conditions for hypsarrhythmia patient's connectivity except 2A. This further indicates that there is a difference in connectivity between hypsarrhythmia and non-hypsarrhythmia patients (Table 4).

To test, if the effect of the patient response to drug may affect the connectivity results, another analysis is conducted to view responders and non-responders in hypsarrhythmia patients and responders in non-hypsarrhythmia patients. Non-responders for non-hypsarrhythmia patients are not included because there was only one patient, who did not have a post-analysis EEG recorded. The calculations are done through a paired t-test. For hypsarrhythmia, statistical significance remains for both responders and non-responders between pre- versus post-conditions. This would indicate that for hypsarrhythmia patients, response of drug treatment did

not affect between pre- versus post- conditions, which may indicate that the drug treatment may have worked to some degree or there may be some other underlying cause. In non-hypsarrhythmia responders, statistical significance remains only for sleep state between pre- versus post- conditions. Statistical significance only in sleep state would indicate that the drug response has statistical effect only in sleep conditions than awake for non-hypsarrhythmia patients (Table 5). However, more patients that can be added for each category would give more of a conclusive support to these statistical results.

Chapter 4: Future Work

1. More Patients Needed

Our results display that each patient has a unique network, network stability persists with increasing temporal window sizes, and long range connections are statistically significant in hypsarrhythmia patients during sleep states. However, one of the bigger concerns is that the analysis produces results that would be more convincing with a larger sample size, especially for the small sample sizes in non-hypsarrhythmia patients. There is also a need for a control group, which would be healthy patients in the same age group such that any discrepancies within infantile spasm patients can be noted. Another unique comparison that can be calculated is the effects of the drugs on the patients with greater patients in each group. An approval by the institutional review board (IRB) has passed to obtain more patient EEG data from CHOC. However, the process to obtain the data and select the clean section of data has been time consuming, and we hope that in the near future this data will be obtained to have more conclusive results in all parts of this paper.

2. Eyeblink and Eye Movement Calculations

Another problem that has not been thoroughly addressed in this paper is the issue of eyeblink and eye movement affecting a large portion of the frontal electrodes, primarily Fp1 and Fp2. This process of determining eyeblinks and eye movements were avoided due to the time consuming nature of locating each movement, and the purpose of this paper was to prove if the connectivity results would be worthy for future analysis. The UCLA data has no electrooculography (EOG) recordings to view eye blinks/movements, and an algorithm needs to be researched to determine if eyeblinks or eye movements may factor into the results. We

attempted an algorithm based on Klein et al. [31]; however, this approach did not appear to work well on the results as the number of eyeblink seconds expected to be removed did not match this algorithm. Another approach is to have the epileptologist determine sections of data that are greatly affected by eye movements. The CHOC data does have EOG recordings, and have to be implemented into the current algorithm to remove any eye movement artifacts.

3. Minimum Spanning Tree and Graph Theory on EEG

Post-processing techniques to quantitatively assess brain networks should further be applied through minimum spanning tree and graph theory on EEG. Understanding of minimum spanning tree (MST) was derived from Boersma et al and Tewarie et al [32, 33]. In MST, a node is defined as an electrode (N) and a link is defined as a relationship between two electrodes. As described by Tewarie et al., MST is a sub-network that connects all nodes while minimizing link weights and without forming loops [33, 34, 35]. Graph theory in EEG incorporates network measures based on average connectivity pairs [33, 36]. From both MST and graph theory, certain post-processing values can be obtained that define the respective networks and these values have relationships with the other network measures [33]. Clustering coefficient analysis from graph theory has been shown to be inversely related to leaf fraction in MST [33]. Another comparison is viewing the results from path length of graph theory that is directly related to diameter in MST [33]. Comparing graph theory on EEG and minimum spanning tree would give more convincing evidence that the results shown are as expected.

Preliminary work was calculated on MST with post-processing values. The values and results calculated display promising results in methods; however, future work and larger sample is required to make a reach a convincing conclusion.

4. More Processes to Differentiate Hypsarrhythmia and Non-Hypsarrhythmia

Although viewing the connectivity between hypsarrhythmia and non-hypsarrhythmia patients has convincing results, viewing the amplitudes and connectivity results over multiple frequency bands may provide interesting conclusions. With the knowledge that hypsarrhythmia patients have EEG that has high amplitude, disorganized, and independent spikes [1], approaches to differentiate hypsarrhythmia include evaluating connectivity, amplitude, and connectivity over various frequency bands. This paper evaluated the connectivity portion of observations. Amplitude measurements of EEG would be another viewable result. Spreading the data over various frequency bands would be able to notice more unique variations in the connectivity that broadband data may overlook. Frequency bands that would have interesting results would be the delta (0.5-4 Hz), theta (4-8 Hz), alpha (8-12 Hz), beta (12-20 Hz), and gamma (20-50 Hz) [15]. Viewing connectivity in the broadband spectrum, amplitude measurements, and connectivity in various frequency bands would provide different approaches to same question.

References

[1] Pavone P, Striano P, Falsaperla R, Pavone L, Ruggieri M. Infantile spasms syndrome, West syndrome and related phenotypes: What we know in 2013. *Brain and Development*. 2014;36(9):739-751. doi:10.1016/j.braindev.2013.10.008.

[2] Shields W. Diagnosis of Infantile Spasms, Lennox-Gastaut Syndrome, and Progressive Myoclonic Epilepsy. *Epilepsia*. 2004;45(s5):2-4. doi:10.1111/j.0013-9580.2004.05002.x.

[3] Shields W. Infantile Spasms: Little Seizures, BIG Consequences. *Epilepsy Currents*. 2006;6(3):63-69. doi:10.1111/j.1535-7511.2006.00100.x.

[4] Caraballo RH, Fejerman R, Bernardina BD. Epileptic spasms in clusters without hypsarrhythmia. Epileptic disorders. 2003;5:109–113.

[5] Tsao C. Current trends in the treatment of infantile spasms. *Neuropsychiatric Disease and Treatment*. 2009:289. doi:10.2147/ndt.s4488.

[6] Hrachovy R, Frost J. Infantile Epileptic Encephalopathy with Hypsarrhythmia (Infantile Spasms/West Syndrome). *Journal of Clinical Neurophysiology*. 2003;20(6):408-425. doi:10.1097/00004691-200311000-00004.

[7] Hrachovy R, Frost J, Kellaway P. Hypsarrhythmia: Variations on the Theme. *Epilepsia*. 1984;25(3):317-325. doi:10.1111/j.1528-1157.1984.tb04195.x.

[8] Burroughs S, Morse R, Mott S, Holmes G. Brain connectivity in West syndrome. *Seizure*. 2014;23(7):576-579. doi:10.1016/j.seizure.2014.03.016.

[9] Greicius M, Kiviniemi V, Tervonen O et al. Persistent default-mode network connectivity during light sedation. *Human Brain Mapping*. 2008;29(7):839-847. doi:10.1002/hbm.20537.

[10] Horovitz S, Braun A, Carr W et al. Decoupling of the brain's default mode network during deep sleep. *Proceedings of the National Academy of Sciences*. 2009;106(27):11376-11381. doi:10.1073/pnas.0901435106.

[11] Bathelt J, O'Reilly H, Clayden J, Cross J, de Haan M. Functional brain network organisation of children between 2 and 5years derived from reconstructed activity of cortical sources of high-density EEG recordings. *NeuroImage*. 2013;82:595-604. doi:10.1016/j.neuroimage.2013.06.003.

[12] Chu C, Tanaka N, Diaz J et al. EEG functional connectivity is partially predicted by underlying white matter connectivity. *NeuroImage*. 2015;108:23-33. doi:10.1016/j.neuroimage.2014.12.033.

[13] Wang Y, Ng W, Ng K, Yu K, Wu T, Li X. An Electroencephalography Network and Connectivity Analysis for Deception in Instructed Lying Tasks. *PLoS ONE*. 2015;10(2):e0116522. doi:10.1371/journal.pone.0116522.

[14] Kramer M, Eden U, Cash S, Kolaczyk E. Network inference with confidence from multivariate time series. *Physical Review E*. 2009;79(6). doi:10.1103/physreve.79.061916.

[15] Chu C, Kramer M, Pathmanathan J et al. Emergence of Stable Functional Networks in Long-Term Human Electroencephalography. *Journal of Neuroscience*. 2012;32(8):2703-2713. doi:10.1523/jneurosci.5669-11.2012.

[16] Alonso J, Mañanas M, Romero S, Rojas-Martínez M, Riba J. Cross-conditional entropy and coherence analysis of pharmaco-EEG changes induced by alprazolam. *Psychopharmacology*. 2011;221(3):397-406. doi:10.1007/s00213-011-2587-7.

[17] Subha D, Joseph P, Acharya U R, Lim C. EEG Signal Analysis: A Survey. *J Med Syst*. 2008;34(2):195-212. doi:10.1007/s10916-008-9231-z.

[18] AND G, LAYNE S. Dimensionality of the Human Electroencephalogram. *Annals of the New York Academy of Sciences*. 1987;504(1 Perspectives):62-87. doi:10.1111/j.1749-6632.1987.tb48726.x.

[19] Cohen M. *Analyzing Neural Time Series Data*.

[20] Bartlett M. On the Theoretical Specification and Sampling Properties of Autocorrelated Time-Series. *Supplement to the Journal of the Royal Statistical Society*. 1946;8(1):27. doi:10.2307/2983611.

[21] Fisher R. Frequency Distribution of the Values of the Correlation Coefficient in Samples from an Indefinitely Large Population. *Biometrika*. 1915;10(4):507. doi:10.2307/2331838.

[22] Tukey J. *Exploratory Data Analysis*. Reading, Mass.: Addison-Wesley Pub. Co.; 1977.

[23] Massey F. The Kolmogorov-Smirnov Test for Goodness of Fit. *Journal of the American Statistical Association*. 1951;46(253):68. doi:10.2307/2280095.

[24] Mathworks.com. Two-sample Kolmogorov-Smirnov test - MATLAB kstest2. 2015. Available at: http://www.mathworks.com/help/stats/kstest2.html.

[25] Eeg.sourceforge.net. Description of elec_distance. 2015. Available at: http://eeg.sourceforge.net/doc_m2html/bioelectromagnetism/elec_distance.html.

[26] Bronzino J, Peterson D. *Biomedical Signals, Imaging, And Informatics*. Boca Raton, FL: CRC Press; 2015.

[27] Mathworks.com. N-way analysis of variance - MATLAB anovan. 2015. Available at: http://www.mathworks.com/help/stats/anovan.html.

[28] Mathworks.com. Multiple comparison test - MATLAB multcompare. 2015. Available at: http://www.mathworks.com/help/stats/multcompare.html.

[29] Multiple Comparison Procedures. *Wiley Series in Probability and Statistics*. 1987. doi:10.1002/9780470316672.

[30] Mathworks.com. One-sample and paired-sample t-test - MATLAB ttest. 2015. Available at: http://www.mathworks.com/help/stats/ttest.html.

[31] Bonilha L, Tabesh A, Dabbs K et al. Neurodevelopmental alterations of large-scale structural networks in children with new-onset epilepsy. *Human Brain Mapping*. 2014;35(8):3661-3672. doi:10.1002/hbm.22428.

[32] Boersma M, Smit D, Boomsma D, De Geus E, Delemarre-van de Waal H, Stam C. Growing Trees in Child Brains: Graph Theoretical Analysis of Electroencephalography-Derived Minimum Spanning Tree in 5- and 7-Year-Old Children Reflects Brain Maturation. *Brain Connectivity*. 2013;3(1):50-60. doi:10.1089/brain.2012.0106.

[33] Tewarie P, van Dellen E, Hillebrand A, Stam C. The minimum spanning tree: An unbiased method for brain network analysis. *NeuroImage*. 2015;104:177-188. doi:10.1016/j.neuroimage.2014.10.015.

[34] Kruskal J. On the shortest spanning subtree of a graph and the traveling salesman problem. *Proc Amer Math Soc*. 1956;7(1):48-48. doi:10.1090/s0002-9939-1956-0078686-7.

[35] Prim R. Shortest Connection Networks And Some Generalizations. *Bell System Technical Journal*. 1957;36(6):1389-1401. doi:10.1002/j.1538-7305.1957.tb01515.x.

[36] Klein A, Skrandies W. A Reliable Statistical Method to Detect Eyeblink-Artefacts from Electroencephalogram Data Only. *Brain Topogr*. 2013;26(4):558-568. doi:10.1007/s10548-013-0281-2.

Supplementary Figures

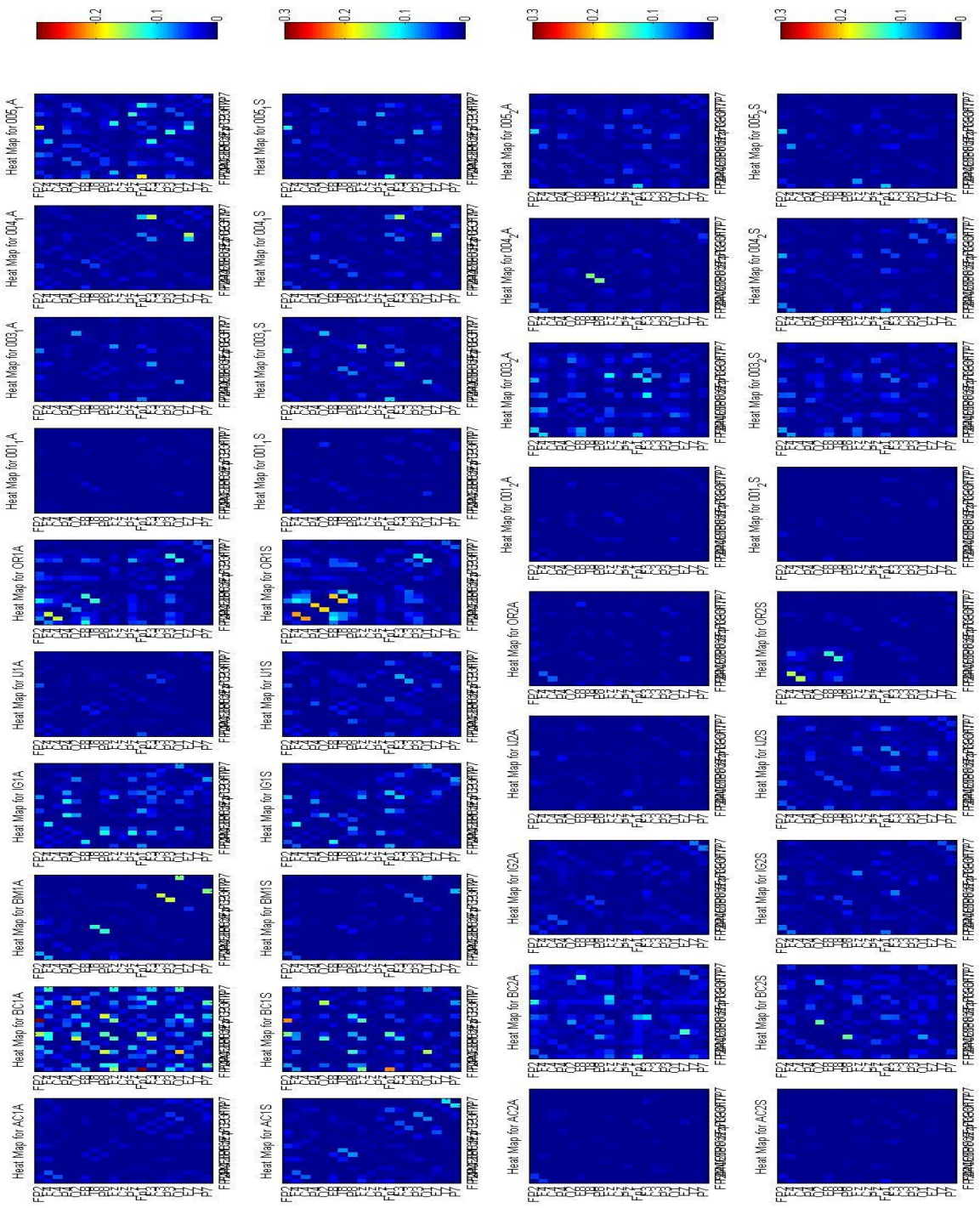

Supplementary Figure 1. Connectivity heat map of Hypsarrhythmia patients, in which color of blue (0) to red (.3) represents the strength of the $\bar{\rho}_{ij}$ between two electrodes. The x and y axis are the electrodes being compared. There are 4 rows of heat maps, which represent the different states/conditions of where it is 1A, 1S, 2A, and 2S, respectively.

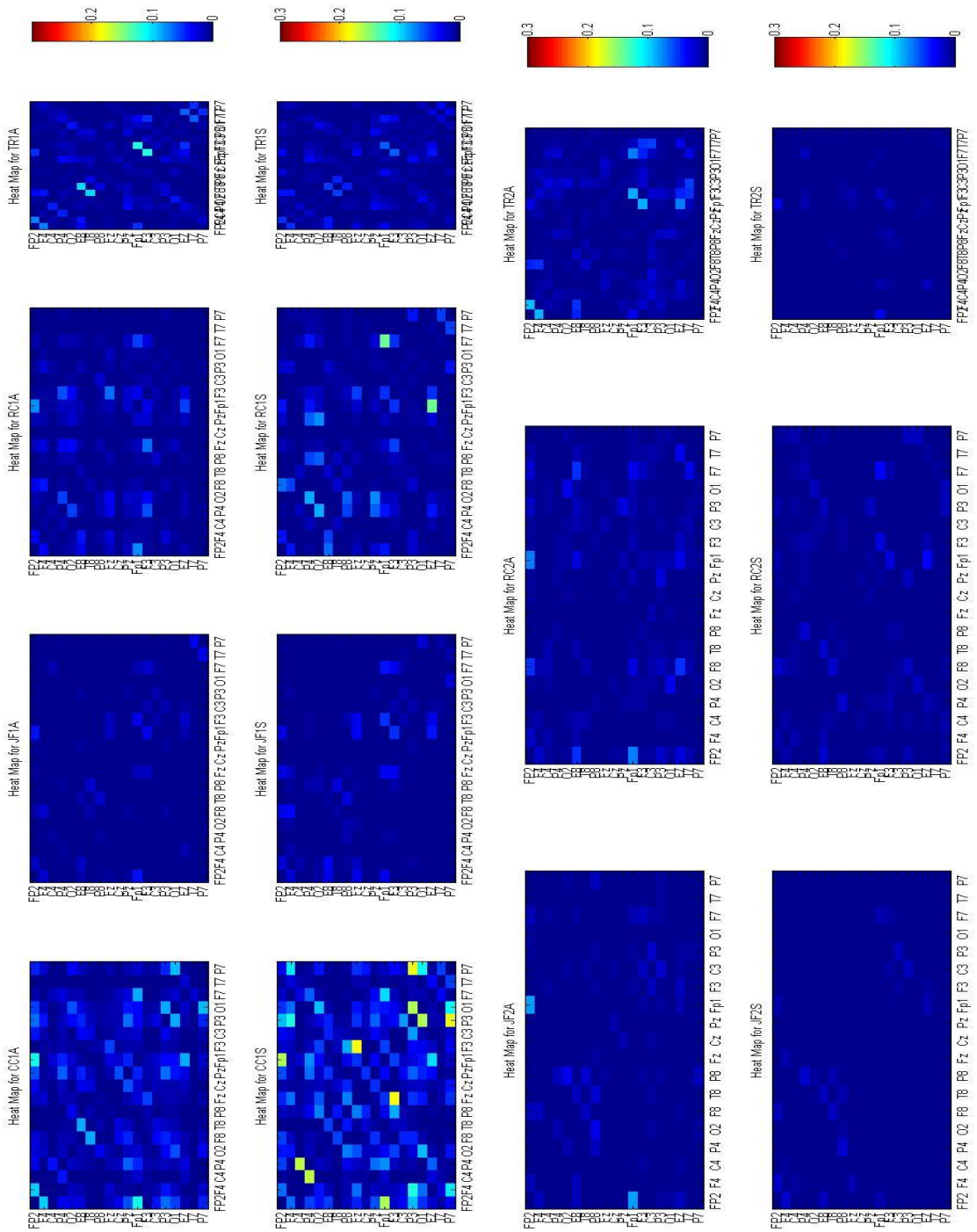

Supplementary Figure 2. Connectivity heat map of Non-Hypsarrhythmia patients, in which color of blue (0) to red (.3) represents the strength of the $\bar{\rho}_{ij}$ between two electrodes. The x and y axis are the electrodes being compared. There are 4 rows of heat maps, which represent the different states/conditions of where it is 1A, 1S, 2A, and 2S, respectively.

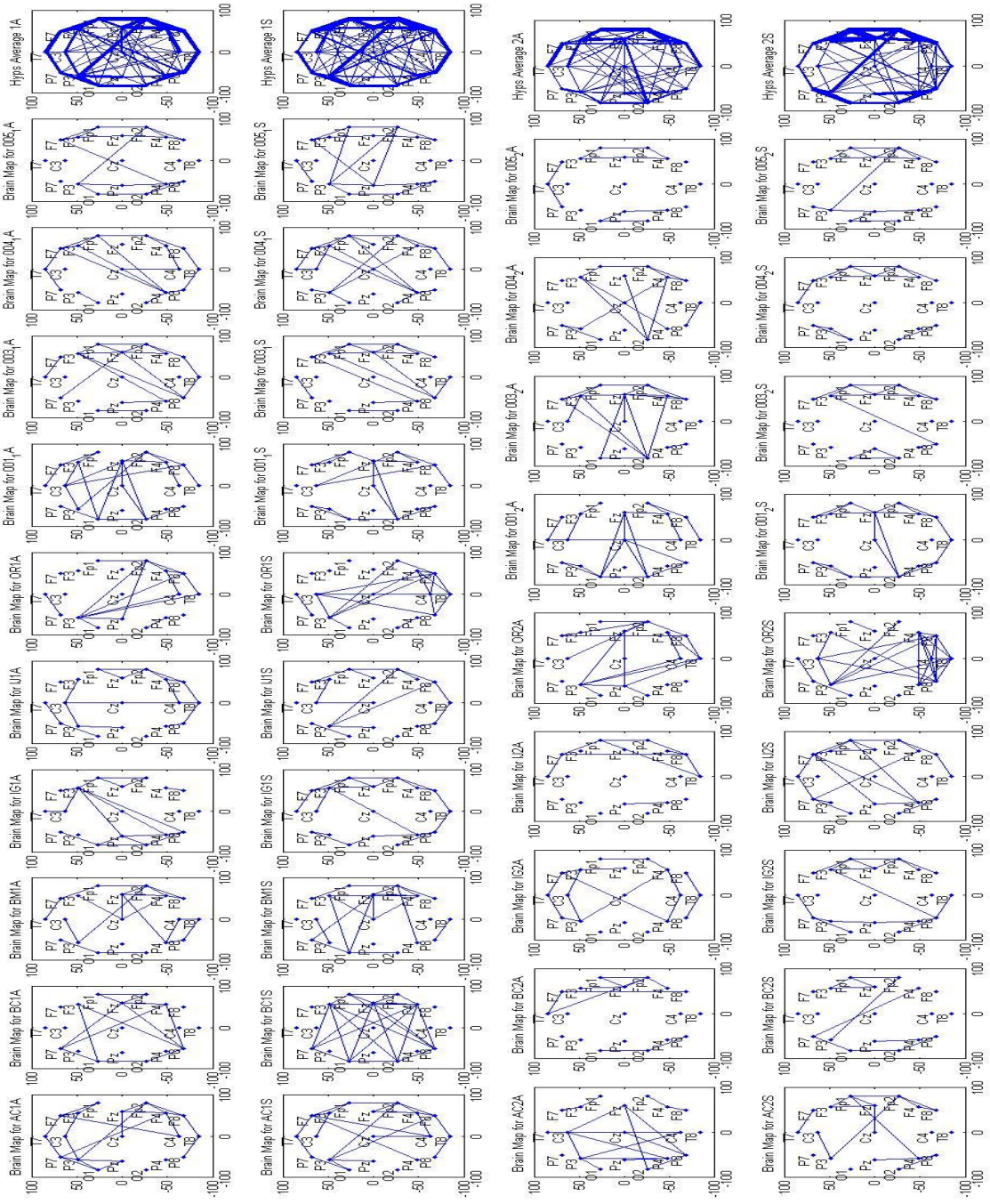

Supplementary Figure 3. Brain map of Hypsarrhythmia patients' connectivity. Each line, for the patient data, is a representation of a strong connection (greater than the 1.5*IQR+Q3 threshold) for the given patient. There are 4 rows of heat maps, which represent the different states/conditions of where it is 1A, 1S, 2A, and 2S, respectively. The last column is an average representation over all patients for that given row. This visual representation displays how unique each individual's connectivity is with only a few commonalities.

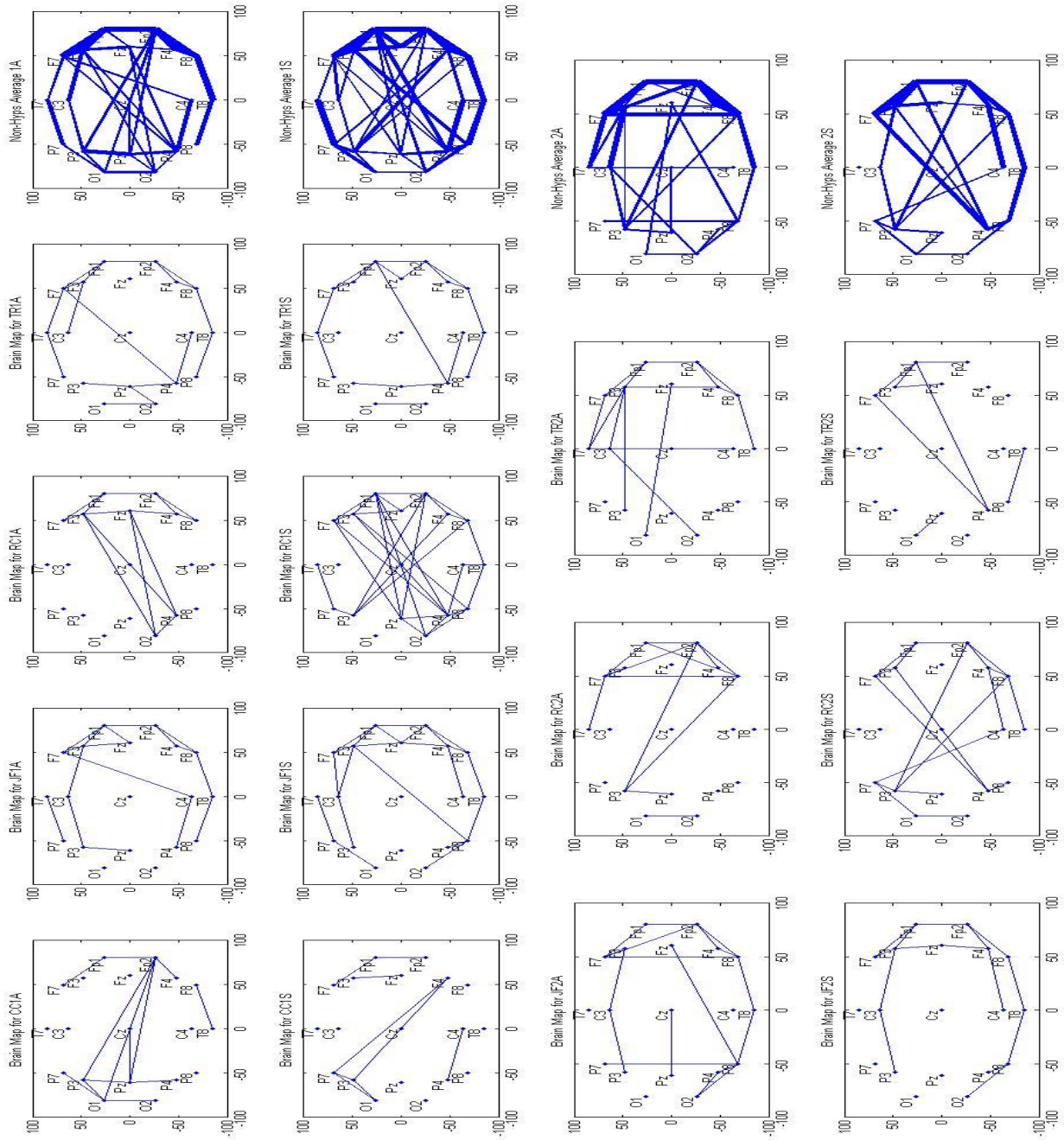

Supplementary Figure 4. Brain map of Non-Hypsarrhythmia patients' connectivity. Each line, for the patient data, is a representation of a strong connection (greater than the 1.5*IQR+Q3 threshold) for the given patient. There are 4 rows of heat maps, which represent the different states/conditions of where it is 1A, 1S, 2A, and 2S, respectively. The last column is an average representation over all patients for that given row. This visual representation displays how unique each individual's connectivity is with only a few commonalities.